AIRCRAFT ACCIDENT REPORT AND EXECUTIVE SUMMARY

			Reference:	CA18/2/3/10070	
Aircraft Registration	ZU-EIJ	**Date of Accident**	7 December 2021	**Time of Accident**	1520Z
Type of Aircraft	Evektor SportStar		**Type of Operation**	Private NTCA (Part 94)	

Pilot-in-command Licence Type	National Pilot Licence	**Age**	49	**Licence Valid**	Yes
Pilot-in-command Flying Experience	**Total Flying Hours**		333.8	**Hours on Type**	48.1

Last Point of Departure	Springs Aerodrome (FASI), Gauteng Province
Next Point of Intended Landing	Springs Aerodrome (FASI), Gauteng Province
Damage to Aircraft	Destroyed
Location of the accident site with reference to easily defined geographical points (GPS readings if possible)	
Bajadam Resort (GPS position: 25°53'52.44" South, 028°42'38.00" East), at an elevation of 4 740 feet (ft)	
Meteorological Information	Strong winds were encountered while flying over the Bronkhorstspruit Dam

Number of People On-board	1 + 0	**Number of People Injured**	0	**Number of People Killed**	1	**Other (On Ground)**	0

Synopsis

On Tuesday afternoon, 7 December 2021, a pilot on-board an Evektor SportStar light aircraft with registration ZU-EIJ took off on a private flight from Springs Aerodrome (FASI) in Gauteng province with the intention to fly over Bronkhorstspruit Dam and, thereafter, land back at FASI. The pilot was accompanied by another pilot on-board an aircraft with registration ZU-AZY and who had a passenger with him. The flights were conducted under the provisions of Part 94 of the Civil Aviation Regulations (CAR) 2011 as amended.

According to the eyewitnesses who were near the dam around the time of the accident, they saw the aircraft flying over the dam from the north towards the south. Something bluish in colour detached from the aircraft fuselage while it was flying over the dam, whereafter, the aircraft was seen twirling in the sky while descending before it impacted the terrain, which was an open field on the southern side of the dam. The outer section of the left wing that failed was located approximately 100 metres (m) from the main wreckage and closer to the water line.

Following the accident of the ZU-EIJ, the pilot of the ZU-AZY aircraft diverted to Kitty Hawk Aerodrome (FAKT) where he landed safely.

Probable cause			
The pilot lost control of the aircraft following the structural failure of the outer left-wing main spar, located 125 centimetres (cm) from the wing tip. The failure was associated with an exceedingly high wing load whilst flying in turbulent conditions, caused by the outflow of a nearby thunderstorm cell. **Contributory factors** (i) The two pilots continued with their flight in extremely turbulent conditions. They had the option to change their intended destination or opt to return to their take-off aerodrome, weather permitting. (ii) The pilots were aware of the thunderstorm activity over the Gauteng province at the time, yet they opted to proceed with the flight.			
SRP date	13 December 2022	Publication date	19 December 2022

Occurrence Details

Reference Number	**:** CA18/2/3/10070
Occurrence Category	**:** Accident (Category 1)
Type of Operation	**:** Operation of Non-type Certificated Aircraft (Part 94)
Name of Operator	**:** Private
Aircraft Registration	**:** ZU-EIJ
Aircraft Make and Model	**:** Evektor Aerotechnik A.S., SportStar
Nationality	**:** South African
Place	**:** Bajadam Resort, Bronkhorstspruit Dam, Gauteng Province
Date and Time	**:** 7 December 2021 at 1520Z
Injuries	**:** Fatal
Damage to aircraft	**:** Destroyed

Purpose of the Investigation

In terms of Regulation 12.03.1 of the Civil Aviation Regulations (CAR) 2011, this report was compiled in the interest of the promotion of aviation safety and the reduction of the risk of aviation accidents or incidents and not to apportion blame or liability.

All times given in this report are Co-ordinated Universal Time (UTC) and will be denoted by (Z). South African Standard Time is UTC plus 2 hours.

Investigation Process

The Accident and Incident Investigations Division (AIID) of the South African Civil Aviation Authority (SACAA) was notified of the occurrence on 7 December 2021 at 1715Z. The occurrence was classified as an accident according to Part 12 of the CAR 2011 and the International Civil Aviation Organisation (ICAO) Standard (STD) Annex 13 definitions. Notifications were sent to the State of Design and Manufacturer in accordance with the CAR 2011 Part 12 and ICAO Annex 13 Chapter 4. The State appointed an accredited representative. This was an on-site investigation.

Notes:

1. *Whenever the following words are mentioned in this report, they shall mean the following:*
   Accident — this investigated accident
   Aircraft — the Evektor SportStar involved in this accident
   Investigation — the investigation into the circumstances of this accident
   Pilot — the pilot involved in this accident
   Report — this accident report

2. *Photos and figures used in this report were taken from different sources and may have been adjusted from the original for the sole purpose of improving clarity of the report. Modifications to images used in this report were limited to cropping, magnification, file compression; or enhancement of colour, brightness, contrast; or addition of text boxes, arrows, or lines.*

Disclaimer

This report is produced without prejudice to the rights of the AIID, which are reserved.

Table of Contents

Abbreviation	Description
°	Degrees
°C	Degrees Celsius
AFM	Aircraft Flight Manual
AGL	Above Ground Level
AIID	Accident and Incident Investigations Division
AMO	Aircraft Maintenance Organisation
AMSL	Above Mean Sea Level
AP	Approved Person
ATF	Authority to Fly
Avg	Average
CAR	Civil Aviation Regulations
C of R	Certificate of Registration
cm	Centimetres
CRS	Certificate of Release to Service
CVR	Cockpit Voice Recorder
ft	Feet
FAKT	Kitty Hawk Aerodrome
FASI	Spring Aerodrome
FDR	Flight Data Recorder
g	Normal Acceleration
GPS	Global Positioning System
hPa	Hectopascal
ICAO	International Civil Aviation Organisation
km/h	Kilometres per hour
kt	Knots
kW	Kilowatt
m	Metre(s)
METAR	Meteorological Aerodrome Report
MTOW	Maximum Take-off Weight
nm	Nautical Miles
NPL	National Pilot Licence
NTCA	Non-type Certified Aircraft
PIC	Pilot-in-command
POH	Pilot’s Operating Handbook
QNH	Barometric Pressure Adjusted to Sea Level
SACAA	South African Civil Aviation Authority
SAWS	South African Weather Service
UTC	Co-ordinated Universal Time
VFR	Visual Flight Rules
VHF	Very High Frequency
Z	Zulu (Term for Universal Co-ordinated Time - Zero Hours Greenwich)

1. FACTUAL INFORMATION

1.1 History of Flight

1.1.1 On Tuesday afternoon, 7 December 2021, a pilot on-board an Evektor SportStar light aircraft with registration ZU-EIJ took off on a private flight from Springs Aerodrome (FASI) in Gauteng province with the intention to land back at FASI. The pilot was accompanied by a friend who was flying his own aircraft with registration ZU-AZY (Zenair Zodiac 601HD) and who had a passenger on-board. According to available information, both aircraft took off from FASI at approximately 1430Z. The flights were conducted under the provisions of Part 94 of the Civil Aviation Regulations (CAR) 2011 as amended.

1.1.2 During an interview with the ZU-AZY pilot, he stated that he, together with the ZU-EIJ pilot, assessed the weather conditions in detail before the flight (see Figure 1, which was provided to the investigator by the ZU-AZY pilot) as they had intended to fly towards the Fortuna Dam near Balfour, which was to the south of FASI. However, after take-off, they decided to fly to the north, over the Bronkhorstspruit Dam as the weather conditions were deteriorating towards the south. He indicated that they were flying in a loose formation (some distance apart), and that visibility towards the north was good as he was able to see Bronkhorstspruit Dam after flying over the N12 highway. The ZU-EIJ pilot informed the ZU-AZY pilot that he was going to fly past them to their left. At this point, they were approximately 5 to 10 nautical miles (nm) south-west of Bronkhorstspruit Dam. The condition of the weather over the dam was clear and seemed calm.

1.1.3 The ZU-AZY pilot further stated that whilst he was flying over the western shore of the dam, the ZU-EIJ pilot reported that he was over the dam wall. At this stage, the ZU-AZY pilot still had sight of the ZU-EIJ aircraft. Whilst flying over the ridge to the north of the dam, the ZU-AZY pilot turned east and, at that stage, his passenger stated that he observed an object falling from the sky. After the pilot had enquired about the direction at which the part came from, they flew to the south and over the ridge. At this point, the ZU-AZY pilot could see waves on the surface of the dam. He radioed the ZU-EIJ pilot several times, but he was unable to establish communication. As they flew over the ridge, they encountered extremely turbulent conditions.

1.1.4 When the ZU-AZY aircraft was overhead the “crash site”, he tried to lower the right wing to have a better view of the site. However, the turbulence at that point was severe and he could not complete the manoeuvre or view the “crash site”. He then turned to the right as he wanted to orbit the site, but he could only manage to slightly bank to the right to get out of the turbulence. He stated that every time he turned the aircraft, it felt as if the turbulence was going to overturn it (the aircraft). He stated that he intended to return to FASI, but the weather conditions had suddenly deteriorated towards the south; he then decided to divert to Kitty Hawk Aerodrome (FAKT) where he landed the aircraft safely.

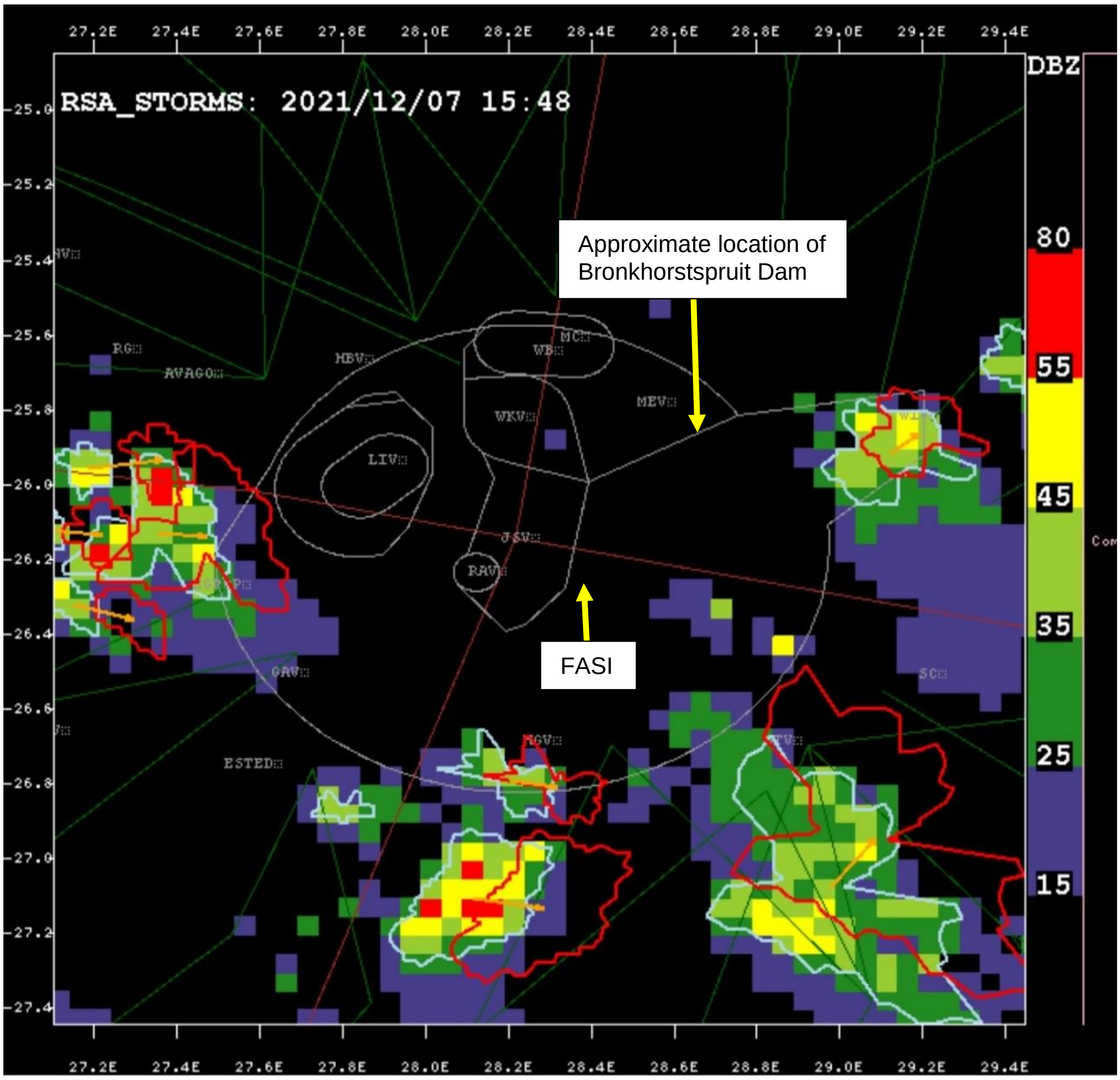

Figure 1: Weather radar information for 7 December 2021 at 1348Z. (Source: ZU-AZY pilot)

1.1.5 According to eyewitnesses who were next to the dam, they stated that they saw the accident aircraft flying over the dam from the north to the south (of the dam). They then saw something bluish in colour detaching from the aircraft fuselage whilst it was flying over the dam, where after the pilot most probably lost control of the aircraft. At the time, a strong wind was blowing in the area. The aircraft was seen twirling in the sky whilst descending, and later impacted terrain, which was an open field on the southern side of the dam. The outer section of the left wing that failed was located approximately 100 metres (m) from the main wreckage and closer to the water line. The pilot was fatally injured in the accident, and the aircraft was destroyed during the impact sequence.

1.1.6 The accident occurred during daylight at Bajadam Resort at Global Positioning System (GPS) co-ordinates determined to be 25°53'52.44" South, 028°42'38.00" East, at an elevation of 4 740 feet (ft).

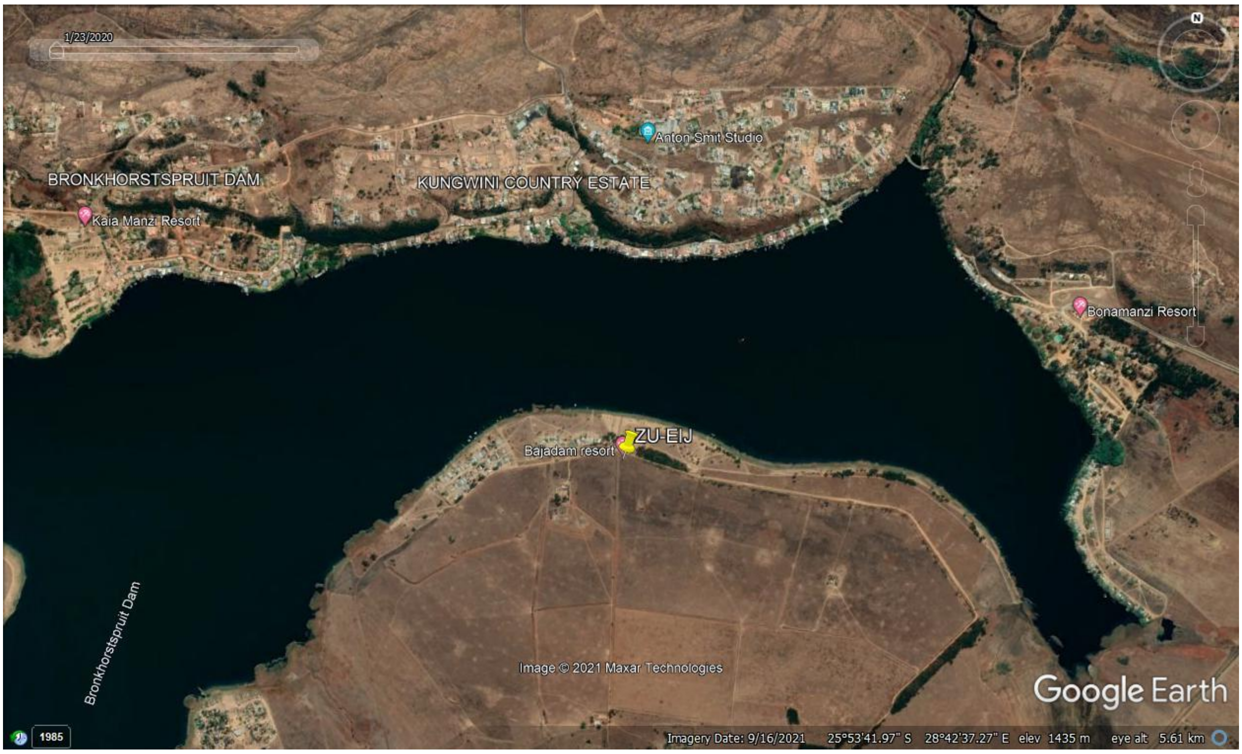

Figure 2: The position of the accident site indicated by the yellow pin ZU-EIJ. (Source: Google Earth)

1.2 Injuries to Persons

Injuries	Pilot	Crew	Pass.	Total On-board	Other
Fatal	1	-	-	1	-
Serious	-	-	-	-	-
Minor	-	-	-	-	-
None	-	-	-	-	-
Total	**1**	**-**	**-**	**1**	**-**

Note: Other means people on the ground.

1.3 Damage to Aircraft

1.3.1 The aircraft was destroyed during the accident sequence.

Figure 3: The main wreckage post-accident. (Source: IIC on site)

1.4 Other Damage

1.4.1 None.

1.5 Personnel Information

1.5.1 Pilot-in-command (PIC)

Nationality	South African	Gender	Male	Age	49
Licence Type	National Pilot Licence				
Licence Valid	Yes	Type Endorsed	Yes		
Ratings	None				
Medical Expiry Date	20 June 2022				
Restrictions	Hypertension protocol				
Previous Accidents	None				

Note: Previous accidents refer to past accidents the pilot was involved in, when relevant to this accident.

According to the pilot's logbook, he started flying on 3 July 2007, and on 12 June 2008, he obtained his National Pilot Licence (NPL). He flew until 4 June 2009, at which point he had flown 66.9 hours. He continued to fly until 4 June 2009 when he stopped; hence, his pilot licence lapsed.

On 12 July 2018, he again enrolled as a student pilot and on 2 September 2018, he passed his skills test; the Regulator reissued his National Pilot Licence after he had flown 30.2 hours. During the period 30 June 2021 and 2 July 2021, the pilot conducted his conversion onto the Evektor SportStar after 3.4 dual hours flown with a flight instructor. From 5 July to 11 October 2021 (the last entry in his logbook), he flew 44.7 hours as pilot-in-command (PIC) on the accident aircraft. The accident flight (on 7 December 2021) was his first flight after the flight on 11 October 2021.

Flying Experience:

Total Hours	333.8
Total Past 90 Days	28.4
Total on Type Past 90 Days	28.4
Total on Type	48.1

1.6 Aircraft Information

1.6.1 Evektor SportStar

Figure 4: Evektor SportStar, ZU-EIJ. (Source: B. Snyman)

Source: Evektor SportStar Pilot's Operating Handbook (POH), Pg. 1-4

The Evektor SportStar aircraft is an all-metal low-wing of semi-monocoque structure with two side-by-side seats and a three-wheel landing gear. The wings are of rectangular shape, single spar structure with the auxiliary spar, with suspended ailerons and split wing flaps. Riveting is used for connecting individual structural elements. Fiberglass wing tips are riveted *on the wing ends. The standard powerplant consists of Rotax 912 ULS engine, which produce 73.5 kilowatt (kW) and is fitted with a Woodcomp SR3000, three-blade propeller which is electrically adjustable. The maximum positive load factor is +4g and the maximum negative load factor is -2g.*

Airframe:

Manufacturer/Model	Evektor Aerotechnik A.S./SportStar	
Serial Number	2006-0714	
Year of Manufacture	2006	
Total Airframe Hours (at time of accident)	564.0	
Last Annual Inspection (date & hours)	515.4	7 June 2021
Airframe Hours Since Last Inspection	48.6	
ATF (issue date & expiry date)	16 September 2019	30 September 2022
C of R (issue date) (Present Owner)	30 June 2021	
Operating Category	Production Built	
Type of Fuel Used	Mogas	
MTOW	550kg	

Engine:

Type	Rotax 912 ULS
Serial Number	5647035
Hours Since New	564.0
Hours Since Overhaul	TBO not yet reached

Propeller:

Type	Woodcomp SR3000/3
Serial Number	PT276
Hours Since New	564.0
Hours Since Overhaul	TBO not yet reached

1.7 Meteorological Information

1.7.1 An official weather report was obtained from the South African Weather Service (SAWS). The closest weather station to the accident site is Irene, Pretoria. The weather information entered in the table below was captured at 1500Z at Irene weather station in Centurion.

Wind Direction	285˚	Wind Speed	5 knots	Visibility	+ 10 km
Temperature	27.1˚C	Cloud Cover	5 octas	Cloud Base	3 500ft
Dew Point	13.3˚C	QNH	850hPa		

1.7.2 Satellite image

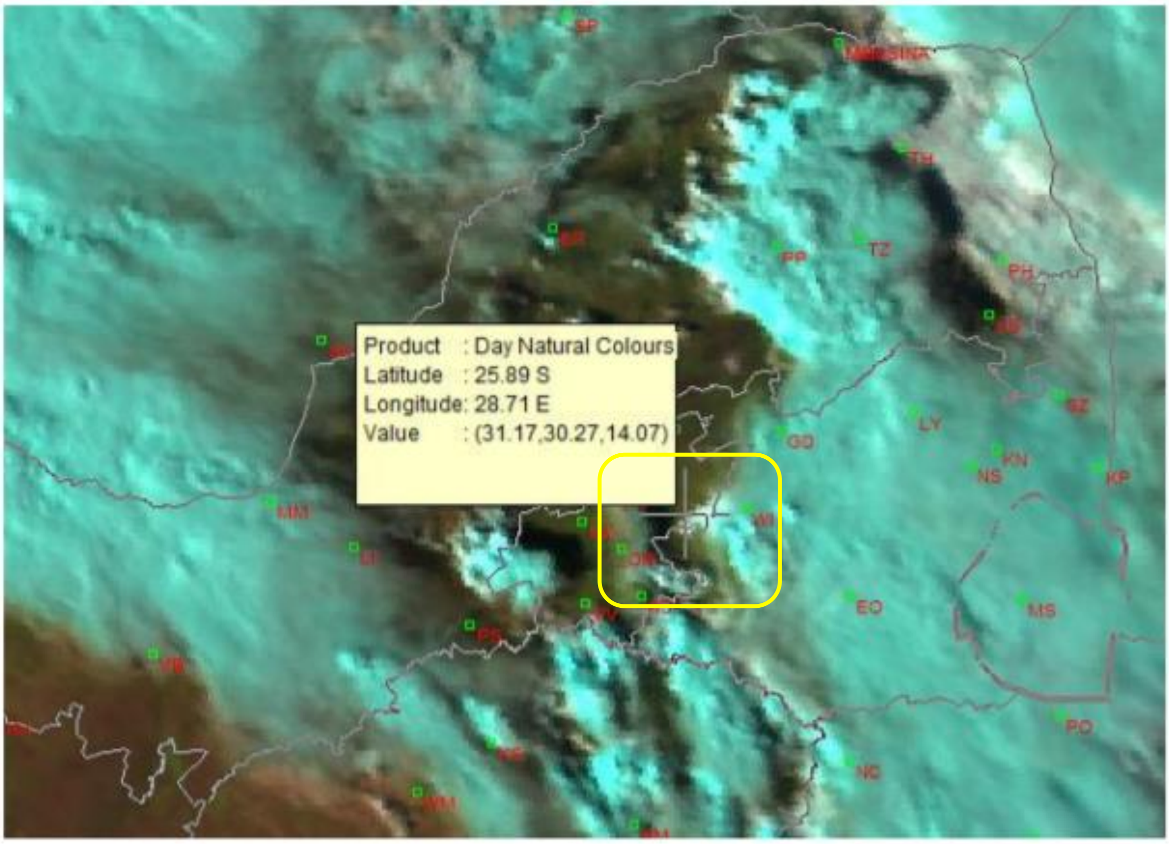

Figure 5: Satellite image of the accident site, marked with a cross in the yellow frame.

The accident site (depicted by a cross) in the satellite image is situated to the west of the thunderstorms, which are visible in the Witbank (FAWI) area (overshooting tops). In the image, it seems possible that cumulus/towering cumulus clouds were present. The eyewitnesses' report did not mention any significant clouds, so it is possible that this development might have been to the immediate east of the dam. It should be noted that turbulence can be expected in any area where cumulus clouds are present.

1.7.3 Wind chart

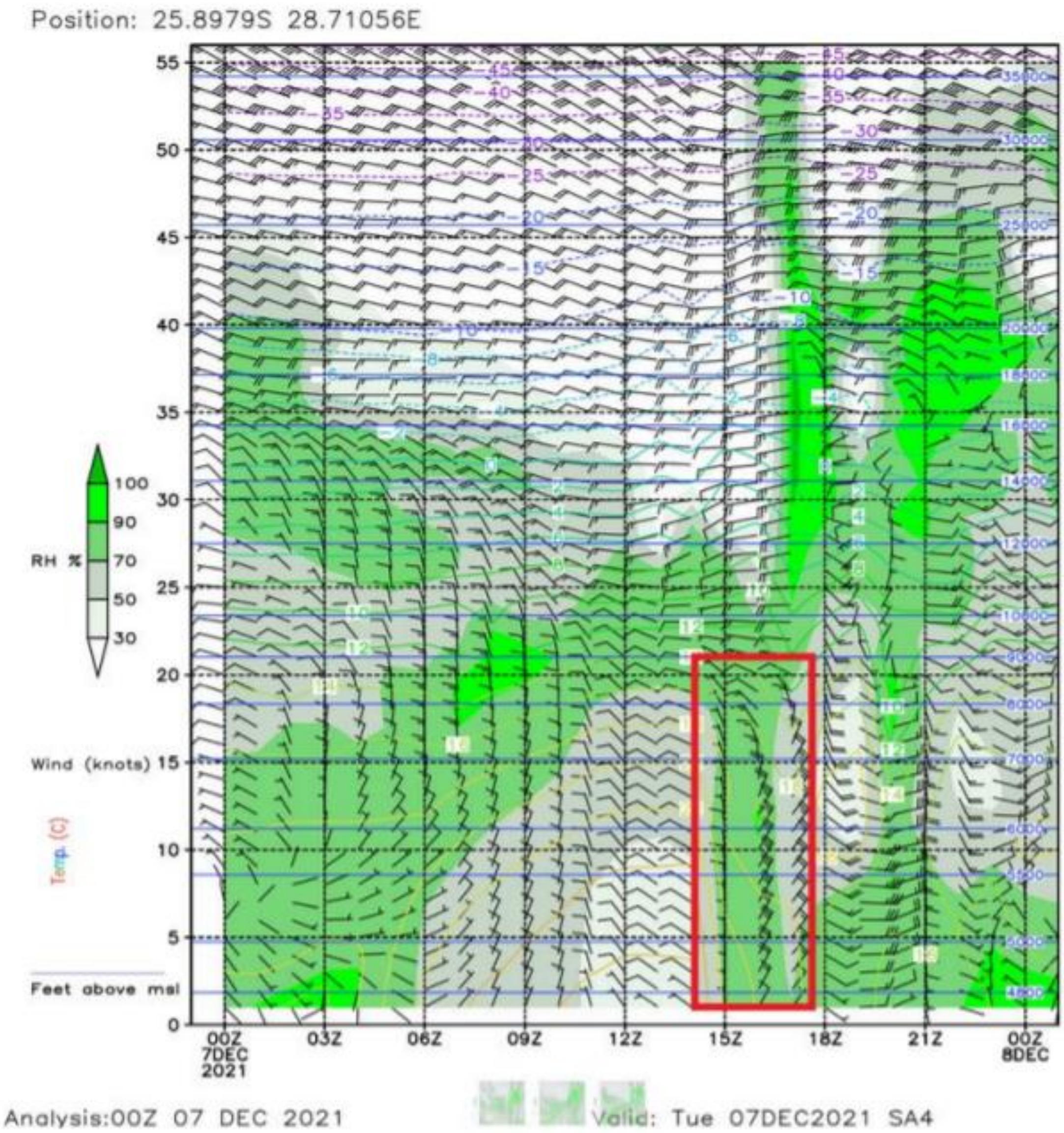

Chart 1: Wind chart

Chart 1 (above) is the Unified Model data for 7 December 2021. The accident occurred at about 1520Z (contained inside the red rectangle). The winds above the surface were expected to pick up to around 25 knots after 1500Z.

1.7.4 Conclusion

It seems possible that cumulus/towering cumulus clouds were present in the area, along with relatively strong winds in the lower levels, which could have caused turbulence.

1.7.5 Weather observation

The investigator was contacted by a person who was fishing in the dam around the time of the accident. He stated that at 1447Z, he decided to take a few photographs of the prevailing weather conditions towards the north, east, south and west.

Figure 6: This photograph was taken at 1447Z in a northerly direction. (Source: Eyewitness)

Figure 7: This photograph was taken at 1447Z in an easterly direction. (Source: Eyewitness)

At 1538Z, he again took several photographs of the prevailing weather conditions. He stated that this was after a gale force wind had passed over the area. He further stated that the conditions went from basically no wind to gale force in about 5 minutes. He reported that the

wind was so strong that he could not take any photographs during that period.
*NOTE: According to the Beaufort wind scale, a gale force wind is a wind between 34 to 40 knots (63 to 75 kilometres per hour).

Figure 8: This photograph was taken at 1538Z in an easterly direction. (Source: Eyewitness)

Figure 9: This photograph was taken at 1538Z in a southerly direction. (Source: Eyewitness)

1.8 Aids to Navigation

1.8.1 The aircraft was equipped with standard navigational equipment as approved by the Regulator (SACAA). There were no records indicating that the navigation system was unserviceable prior to the accident flight.

1.9 Communication

1.9.1 The aircraft was equipped with a standard communication system as approved by the Regulator. There were no recorded defects with the communication system prior to the accident flight.

1.9.2 The ZU-AZY pilot stated that he was in contact with the ZU-EIJ pilot on the very high frequency (VHF) 125.40-Megahertz (MHz). There was no distress call from the ZU-EIJ pilot at any time during the flight.

1.10 Aerodrome Information

1.10.1 The accident did not occur at or near an aerodrome.

1.11 Flight Recorders

1.11.1 The aircraft was neither equipped with a flight data recorder (FDR) or a cockpit voice recorder (CVR), nor was it required by regulation to be fitted to the aircraft type.

1.11.2 A portable Garmin GPS Map 296 with Serial No. 10701101 was on-board the aircraft. The unit was recovered from the accident site. The accident flight data was downloaded, as well as several previous flights (45 active track logs on the unit). The GPS tracking device recorded that the aircraft was on a north-easterly heading at an average ground speed of 91 knots (kt) (168 km/h) and a height of 6 500ft (GPS height). The highest speed that was captured was 114 kt (211 km/h). The average speed in the right turn prior to the failure of the wing was 93 kt (173 km/h), which was measured from the time the aircraft heading changed (commencing with the turn) until the GPS unit stopped recording. The outer section of the left wing failed while the aircraft was still turning.

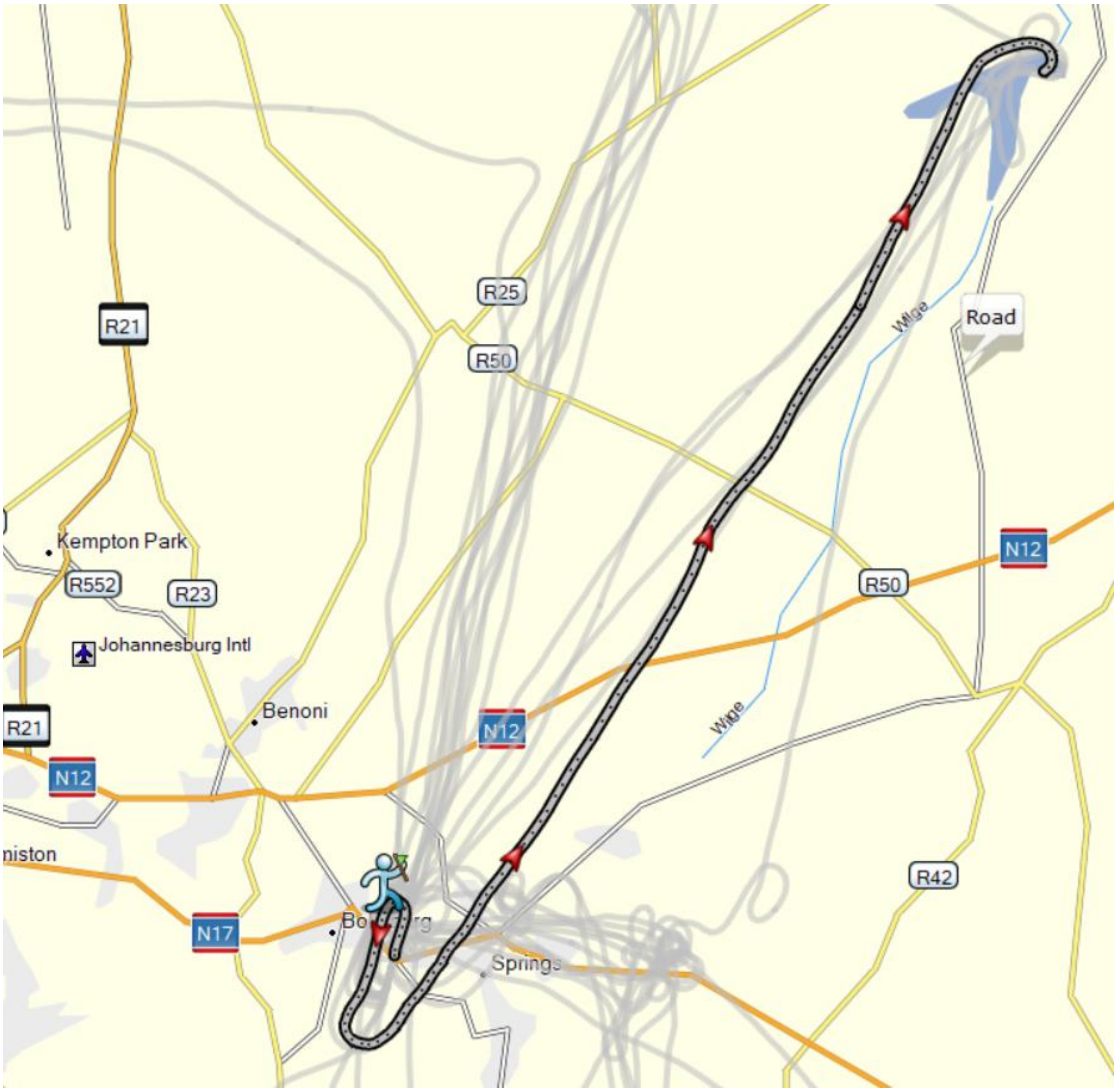

Figure 10: The track that was flown by the pilot. (Source: Data downloaded from the GPS)

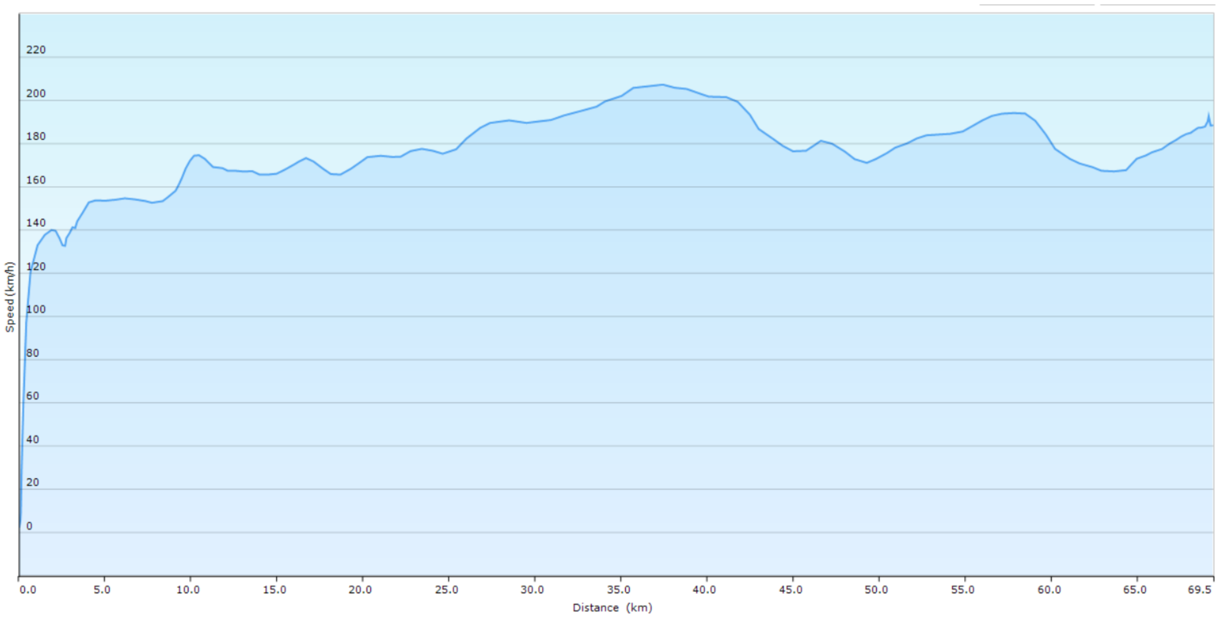

Figure 11: A graph of the flight profile from take-off until the GPS stopped recording.

(Source: Data downloaded from the GPS)

1.11.3 GPS data was downloaded from the unit for the entire accident flight.

Note: The data tables are attached to the report as Appendix A.

1.12 Wreckage and Impact Information

1.12.1 The aircraft impacted the ground on an open field in a westerly direction (255° Magnetic). The aircraft was in a nose-down attitude during ground impact and was described by one of the eyewitnesses as twirling in the air once the outer section of the left wing failed. It was evident from the first ground impact marking and the destruction of the wreckage that the aircraft was out of control during impact. The right-wing assembly was found fractured and was one of the first major components found along the impact line. The inner section of the left-wing remained attached to the fuselage, but was destructed. The entire propeller hub assembly, including the propeller gearbox, had sheared from the engine. The three wooden propeller blades were severed at the hub assembly, which is an indication that the engine was delivering power to the engine on impact with the terrain. The cockpit area was mangled, and all the flight instruments were ripped out of the instrument panel. The fuel tank selector indicated that the left tank was selected at the time of the accident.

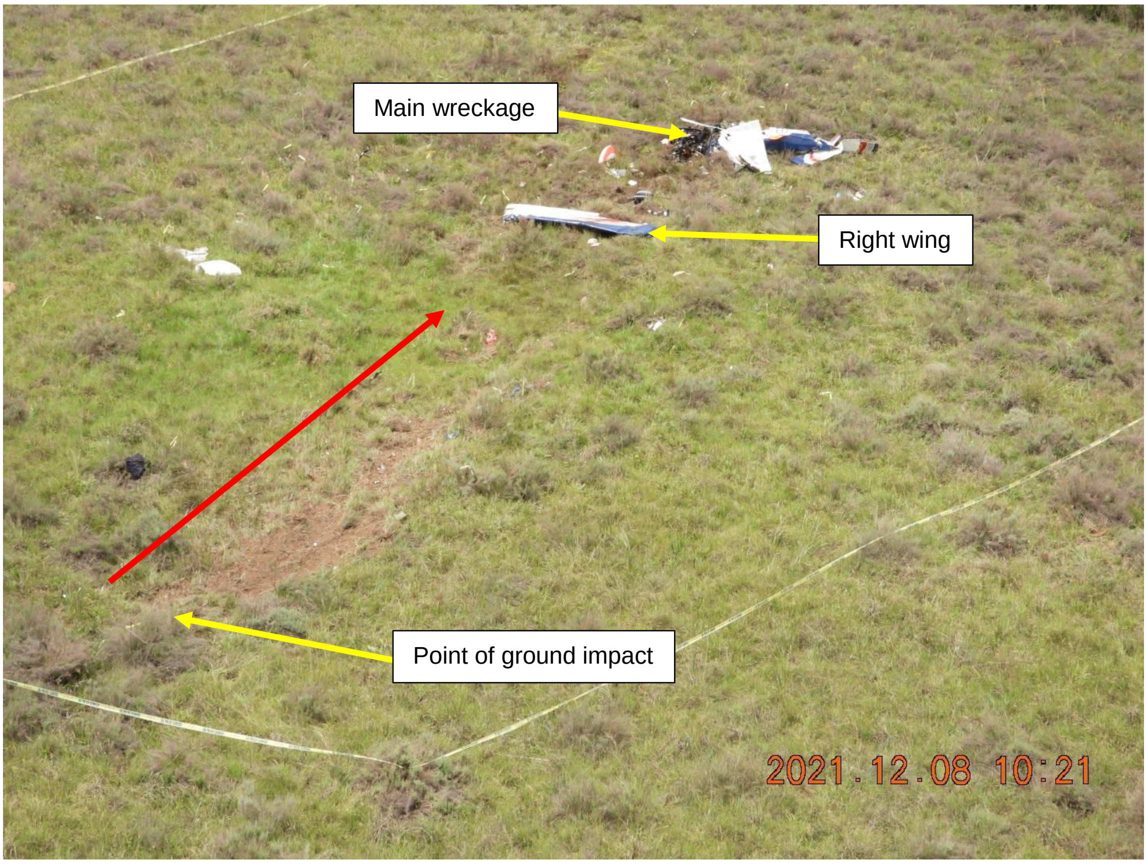

Figure 12: Aerial view of the accident site. The red arrow indicates the direction of impact.

Figure 13: A view of the main wreckage.
(Source: IIC - Photograph was taken on the day of the accident in the afternoon)

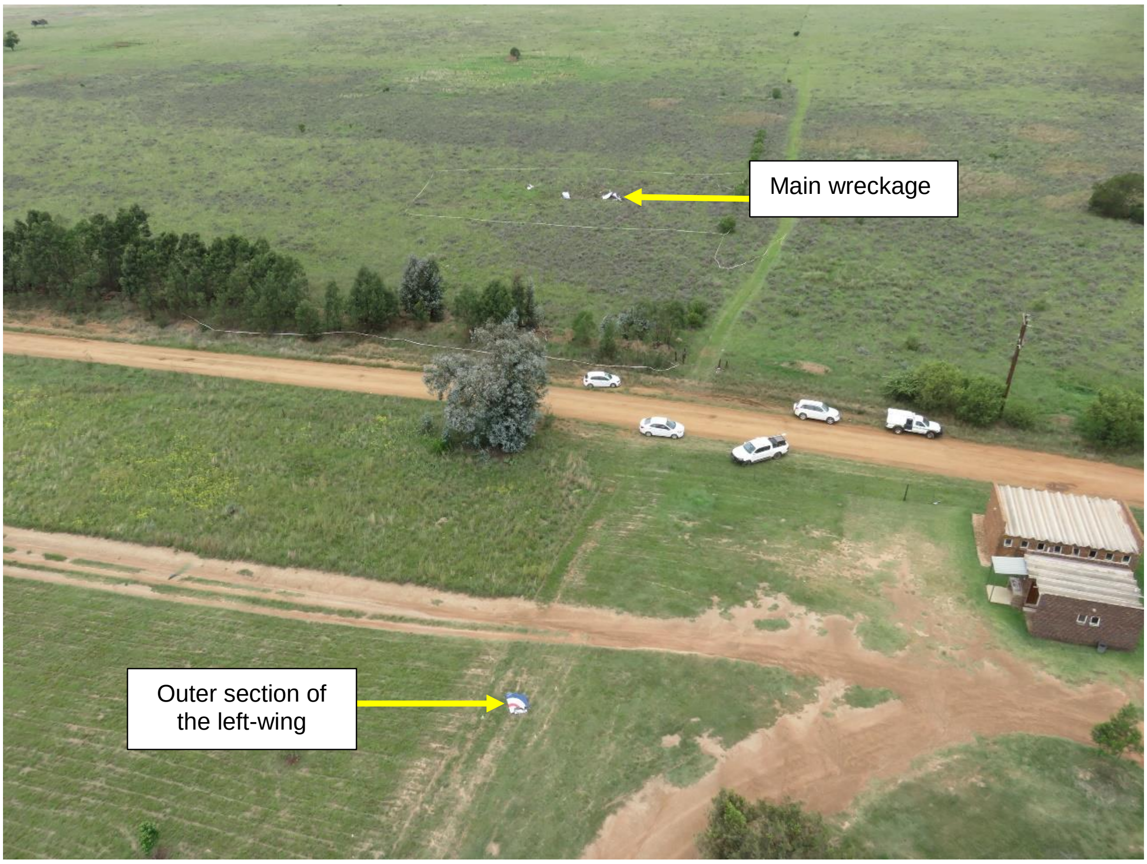

Figure 14: The aerial view showing the main wreckage and the outer section of the left-wing.

Figure 15: The outer section of the left-wing.

1.13 Medical and Pathological Information

1.13.1 The medico-legal post-mortem examination that was performed at the Pretoria Government Mortuary concluded that the cause of death was due to multiple injuries.

1.14 Fire

1.14.1 There was no evidence of a pre- or post-impact fire.

1.15 Survival Aspects

1.15.1 The accident was not survivable as the failure of the outer wing section resulted in the loss of control of the aircraft, followed by the ground impact at a high speed.

1.15.2 The aircraft was not fitted with a ballistic parachute which, according to the Aircraft Flight Manual (AFM), is optional.

1.16 Tests and Research

1.16.1 The entire left wing (both sections) as well as the main wing spar centre section were recovered from the accident site and were sent for metallurgical examination. The laboratory report is attached to this report as Appendix B.

Figure 16: The left wing (both sections) positioned upside down.

Figure 17: The area where the left wing failed is between ribs 8 and 9.

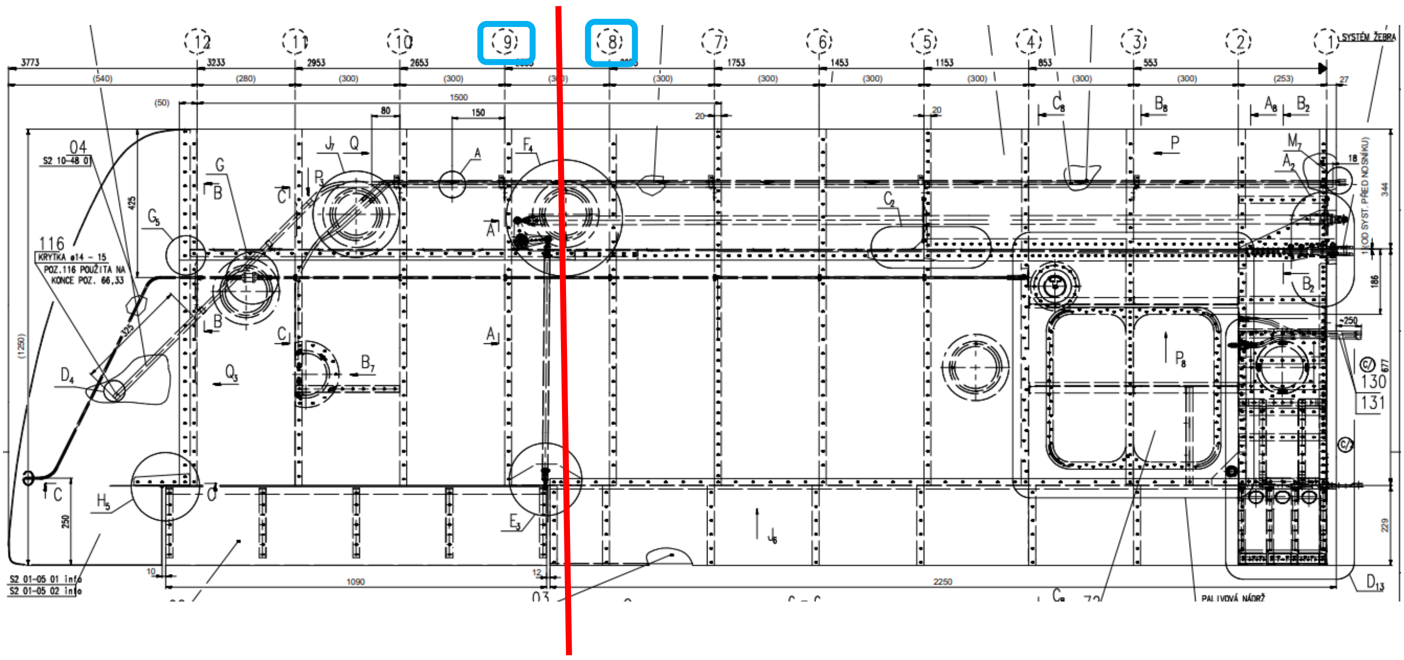

Diagram 1: The red line indicates the area of failure between ribs 8 and 9, looking at the wing from above.

1.17 Organisational and Management Information

1.17.1 This was a private flight conducted under the provisions of Part 94 of the CAR 2011 as amended.

1.17.2 The last annual inspection that was carried out on this aircraft prior to the accident flight was certified on 7 June 2021 at 515.4 airframe hours by an Approved Person (AP). A further 48.6 hours were flown post-inspection.

1.18 Additional Information

1.18.1 Airspeed Limitations

Source: Aircraft Flight Manual, Section 2, Limitations, Pages 2-3 and 2-4

Note: The following extract is from the AFM. It provides the pilot with the airspeed limitations of the aircraft as well as information on the different colour codes on the airspeed indicator. Figure 18 shows the instrument panel layout, which was similar to the cockpit layout of the accident aircraft. The airspeed indicator is visible in the yellow window.

Figure 18: The Instrument panel of a similar aircraft.
(Source: https://alchetron.com/Evektor-SportStar)

SPORTSTAR
FLIGHT MANUAL
Doc. No. S2005FMENKT

Section 2
Limitations

2.1 Introduction

Section 2 contains operation limitation, instrument marking and basic placards necessary for safe operation of airplane and its engine, standard systems and equipment.
Limitation for optional systems and equipment are stated in section 9 – Supplements.

2.2 Airspeed

Airspeed limitations and their meaning for operation are stated in the table below:

	Speed	KIAS	mph IAS	Meaning
V_{NE}	Never exceed speed	146	168	Do not exceed this speed in any operation.
V_{NO}	Maximum structural cruising speed	103	118	Do not exceed this speed, with exception of flight in smooth air, and even then only with increased caution.
V_A	Manoeuvring speed	86	99	Do not make full or abrupt control movement above this speed, because under certain conditions the aircraft may be overstressed by full control movement.
V_{FE}	Maximum flap extended speed	70	81	Do not exceed this speed with the given flap setting.

2.3 Airspeed indicator marking

Airspeed indicator markings and their colour–code significance are shown in the table below:

Marking	Range		Meaning
	KIAS	mph IAS	
Red line	37	43	V_{S0} at maximum weight (flaps in landing position 50°)
White arc	37 – 70	43 – 81	Operating range with extended flaps. Lower limit– V_{S0} at maximum weight (flaps 50°) Upper limit – V_{FE}

October 20, 2005 2–3

Extract 1: Contents from the AFM, Section 2, Limitations, Page 2-3.

Marking	Range		Meaning
	KIAS	mph IAS	
Green arc	42 – 103	49 – 118	Normal operation range Lower limit – V_{S1} at maximum weight (flaps 0°) Upper limit – V_{NO}
Yellow arc	103 – 146	118 – 168	Manoeuvres must be conducted with caution and only in smooth air
Red line	146	168	Maximum speed for all operations – V_{NE}.

2.4 Powerplant

Engine manufacturer:	Bombardier–Rotax GMBH		
Engine type:	ROTAX 912 ULS		
Power:	maximum take–off	100 HP / 73.5 kW	
	maximum continuous	93.8 HP / 69.0 kW	
Engine speed:	maximum take–off	5800 RPM max. 5 minutes	
	maximum continuous	5500 RPM	
	idle	1400 RPM	
Cylinder head temperature:	maximum	135 °C	275 °F
Oil temperature:	maximum	130 °C	266 °F
	optimum operation	90 – 110 °C	190 – 230 °F
Oil pressure:	maximum	7 bar	102 PSI
	minimum	0.8 bar	12 PSI
	optimum operation	2 – 5 bar	29 – 73 PSI
Fuel pressure:	minimum	0.15 bar	2.2 PSI
Fuel grades:	see 2.13, page 2–8		
Oil grades:	see 2.14, page 2–8		
Reducer gear ratio:	2.43 : 1		
Propeller manufacturer:	WOODCOMP s.r.o.		
Propeller type:	KLASSIC 170/3/R 3 blade, composite, on–ground adjustable		
Propeller diameter:	68 in	1700 mm	
Maximum prop speed:	2600 RPM		

NOTE

If installed a different propeller type – see section 9 – Supplements for propeller limitations.

Extract 2: Contents from the AFM, Section 2, Limitations, Page 2-4.

1.18.2 Flight Envelope

Source:
https://www.uavnavigation.com/support/kb/general/general-system-info/flight-envelope

Introduction

1. In aerodynamics, the flight envelope defines operational limits for an aerial platform with respect to maximum speed and load factor given a particular atmospheric density. The flight envelope is the region within which an aircraft can operate safely.

2. If an aircraft flies 'outside the envelope' it may suffer damage; the limits should therefore never be exceeded. The term has also been adopted in other fields of engineering when referring to the behaviour of a system which is operating beyond its normal design specification, i.e., 'outside the flight envelope' (even if the system is not even actually flying).

3. Visual Representation. There are several types of aircraft flight envelope diagrams, normally depicting the relation between one flight parameter and another. The most common diagram includes airspeed (normally expressed in Mach) and flight altitude variation (V-h) or ***airspeed and load variation (V-n)****.*

4. The second diagram, which is the most important and common plot used as it shows structural load limits as a function of airspeed. This flight envelope is normally defined during the design phase. A chart of speed versus load factor (or V-n diagram) is a way of showing the limits of an aircraft's performance. It shows how much load factor can be safely achieved at different airspeeds.

5. The definition and analysis of the V-n diagram is critical during the design of an aircraft as it affects the operation of the aircraft. A manoeuvre or gust of wind may temporarily force an aircraft outside its safe flight envelope and thereby ***cause structural damage endangering flight safety.***

6. The following is a basic V-n diagram (sometimes referred to as a V-g diagram) including the most important features of such diagrams. The diagram does not belong to a specific aircraft. In this example the V-n diagram represents airspeed (horizontal axis) against load factor (vertical axis). In more complex aircraft the diagram may vary.

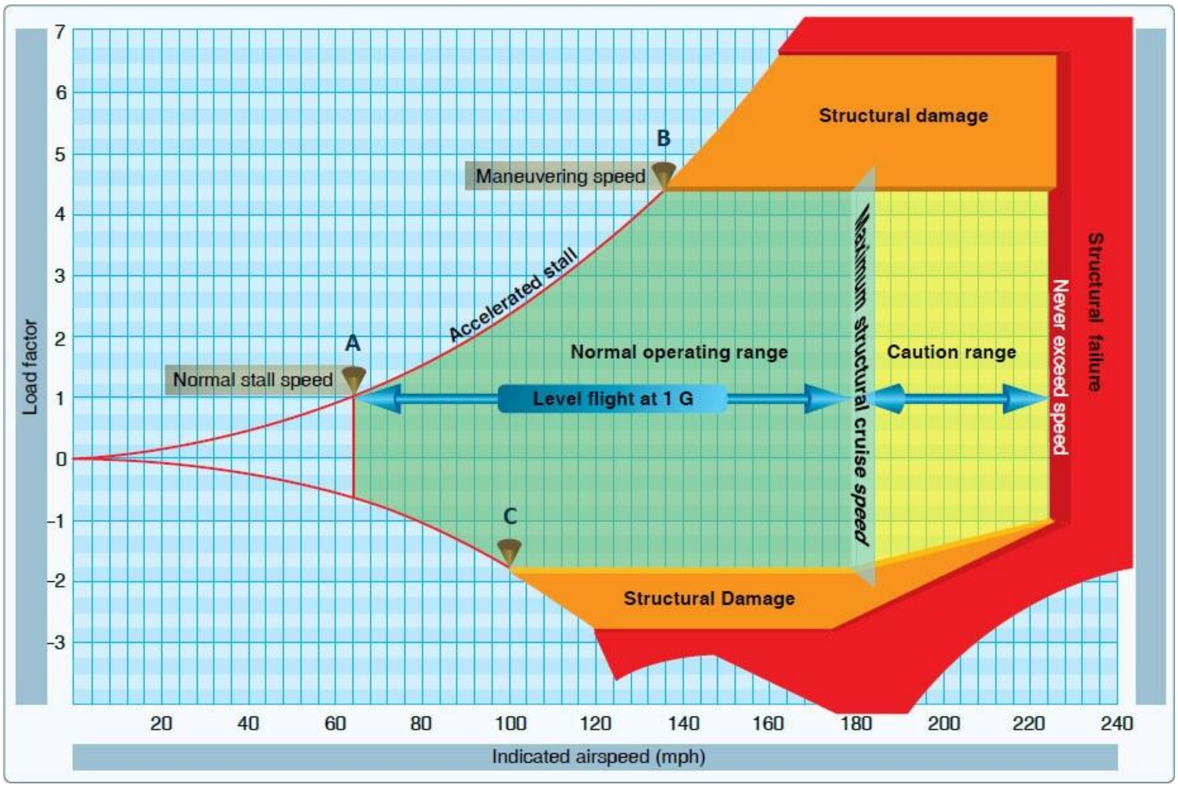

Diagram 2: Typical V-n diagram. (Note: This diagram is not aircraft-specific)

7. Load Factor. An aircraft structure is designed to be able to withstand the forces exerted upon it during flight; together, these forces are calculated as the load factor and may vary depending on the phase of flight; the load factor is defined as the relationship between lift and the weight of the aircraft:

$$n = \frac{L}{W}$$

Where: n = Load factor

L = Lift

W = Weight

The load factor is equal to 1 when the aircraft is static on the ground, with only gravity acting upon it. The load factor can, therefore, be defined as a multiple of gravitational acceleration g.

There are various important features of the V-n diagram:

*8.1. The normal stall speed (**point A**) is defined by the aerodynamic characteristics of the platform. In the example above, the aircraft is capable of developing n=1 (1g) at 62 mph, which is the wing level stall speed of the aircraft.*

*8.2. The intersection of the positive limit of the load factor and the line of maximum lift (**point B**) defines the maximum airspeed that allows full manoeuvrability. This point is called the manoeuvre speed or corner speed. At lower speeds, the structure cannot be overstressed as it will stall before reaching the limit load factor. At the manoeuvre airspeed the aircraft's limit load factor will be reached at the lowest possible airspeed. At higher speeds, possible structural damage may be caused. In the diagram above, the manoeuvring speed is reached in n=4.4g and IAS=137 mph.*

*8.3. The intersection of the negative limit load factor and line of maximum negative lift capability (**point C**) defines the maximum airspeed that allows full manoeuvrability in a negative lift situation. As the graph shows, airspeeds greater than point C provide sufficient negative lift to damage the structure.*

8.4. The airspeed necessary to produce a given negative load factor is higher than that to produce the same positive load factor.

8.5. To ensure structural safety, a maximum structural cruise speed should be defined. It is normally defined as a reference point for every aircraft; in the example above, it is 180mph. Additionally, the diagram defines the never exceed speed or diving speed. This is the maximum speed (normally 1.25 Cruise speed) before the aircraft enters the region where structural failure is possible.

8.6. When an aircraft is operated in the regions called Structural Damage *or* Structural Failure*, unacceptable permanent deformation of the primary structure and a high rate of fatigue may take place.* ***Operation above the limit load factor must therefore be avoided in normal operation.***

1.18.3 Wing Structure

Source: https://www.aircraftsystemstech.com/p/wings-wing-configurations-wings-are.html#:~:text=Currently%2C%20most%20manufactured%20aircraft%20have,from%20a%20variety%20of%20materials

The Wing

The wings of an aircraft are designed to lift it into the air. Their particular design for any given aircraft depends on a number of factors, such as size, weight, use of the aircraft, desired speed in flight and at landing, and desired rate of climb. The wings of aircraft are designated left and right, corresponding to the left and right sides of the operator when seated in the cockpit

Often wings are of full cantilever design. This means they are built so that no external bracing is needed. They are supported internally by structural members assisted by the skin of the aircraft. Other aircraft wings use external struts or wires to assist in supporting the wing and carrying the aerodynamic and landing loads. Wing support cables and struts are generally made from steel. Many struts and their attach fittings have fairings to reduce drag. Short, nearly vertical supports called jury struts are found on struts that attach to the wings a great distance from the fuselage. This serves to subdue strut movement and oscillation caused by the air flowing around the strut in flight.

Aluminium is the most common material from which to construct wings, but they can be wood covered with fabric, and occasionally a magnesium alloy has been used. Moreover, modern aircraft are tending toward lighter and stronger materials throughout the airframe and in wing construction. Wings made entirely of carbon fibre or other composite materials exist, as well as wings made of a combination of materials for maximum strength to weight performance.

The internal structures of most wings are made up of spars and stringers running spanwise and ribs and formers or bulkheads running chordwise (leading edge to trailing edge). The spars are the principle structural members of a wing. They support all distributed loads, as well as concentrated weights such as the fuselage, landing gear, and engines. The skin, which is attached to the wing structure, carries part of the loads imposed during flight. It also transfers the stresses to the wing ribs. The ribs, in turn, transfer the loads to the wing spars.

Wing Spars

Spars are the principal structural members of the wing. They correspond to the longerons of the fuselage. They run parallel to the lateral axis of the aircraft, from the fuselage toward the tip of the wing, and are usually attached to the fuselage by wing fittings, plain beams, or a truss.

Spars may be made of metal, wood, or composite materials depending on the design criteria of a specific aircraft. Currently, most manufactured aircraft have wing spars made of solid extruded aluminium or aluminium extrusions riveted together to form the spar. The increased use of composites and the combining of materials should make airmen vigilant for wings spars made from a variety of materials. Figure 19 shows examples of metal wing spar cross-sections.

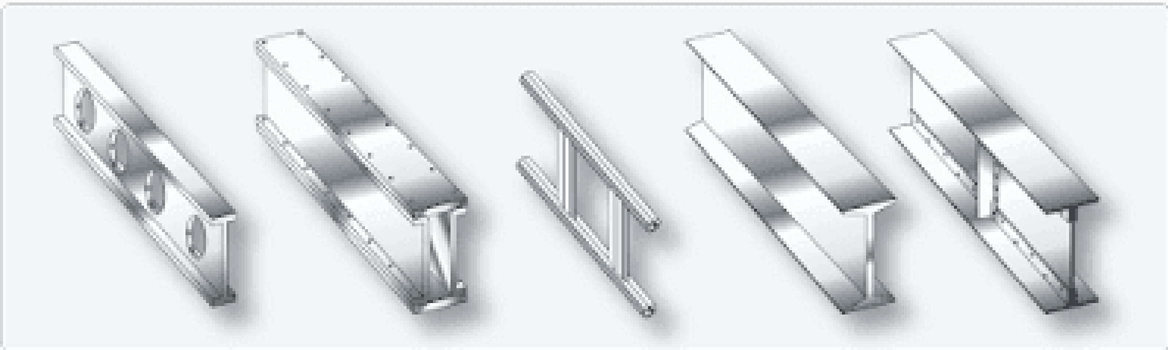

Figure 19: Examples of metal wing spar shapes.

In an I–beam spar, the top and bottom of the I–beam are called the caps and the vertical section is called the web. The entire spar can be extruded from one piece of metal but often it is built up from multiple extrusions or formed angles. The web forms the principal depth portion of the spar and the cap strips (extrusions, formed angles, or milled sections) are attached to it. Together, these members carry the loads caused by wing bending, with the caps providing a foundation for attaching the skin. Although the spar shapes in Figure 11 are typical, actual wing spar configurations assume many forms. For example, the web of a spar may be a plate, or a truss. It could be built up from lightweight materials with vertical stiffeners employed for strength.

As a rule, a wing has two spars. One spar is usually located near the front of the wing, and the other about two-thirds of the distance toward the wing's trailing edge. Regardless of type, the spar is the most important part of the wing. When other structural members of the wing are placed under load, most of the resulting stress is passed on to the wing spar.

False spars are commonly used in wing design. They are longitudinal members like spars but do not extend the entire spanwise length of the wing. Often, they are used as hinge attach points for control surfaces, such as an aileron spar.

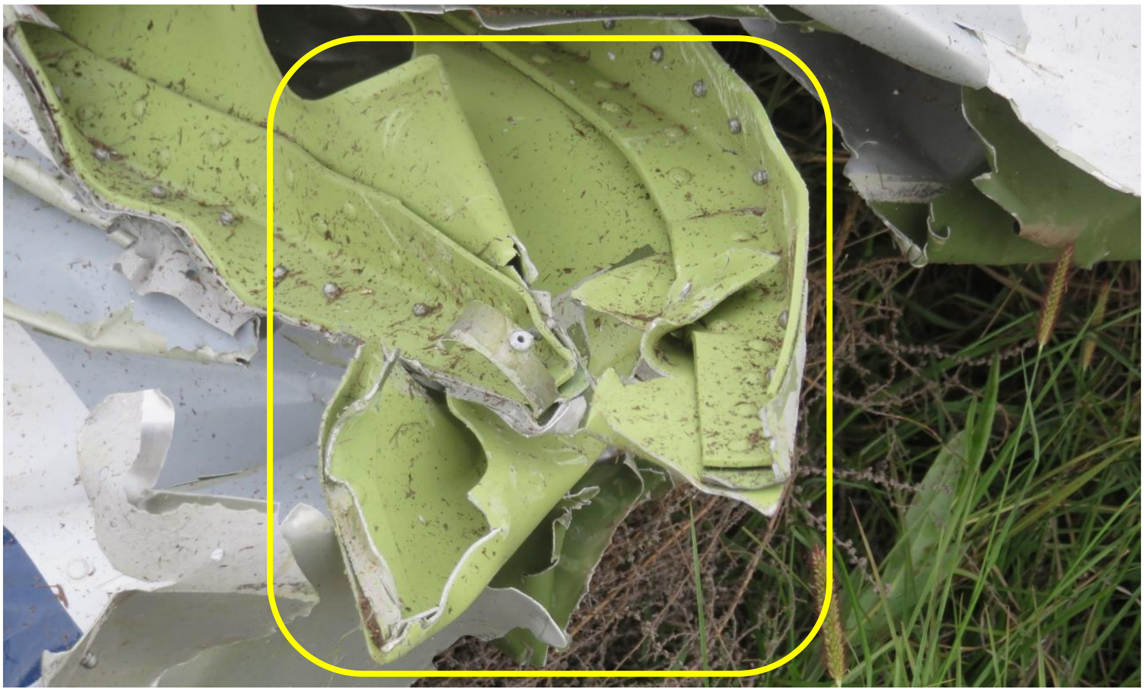

Figure 20: A view of the failed main spar on the left wing.

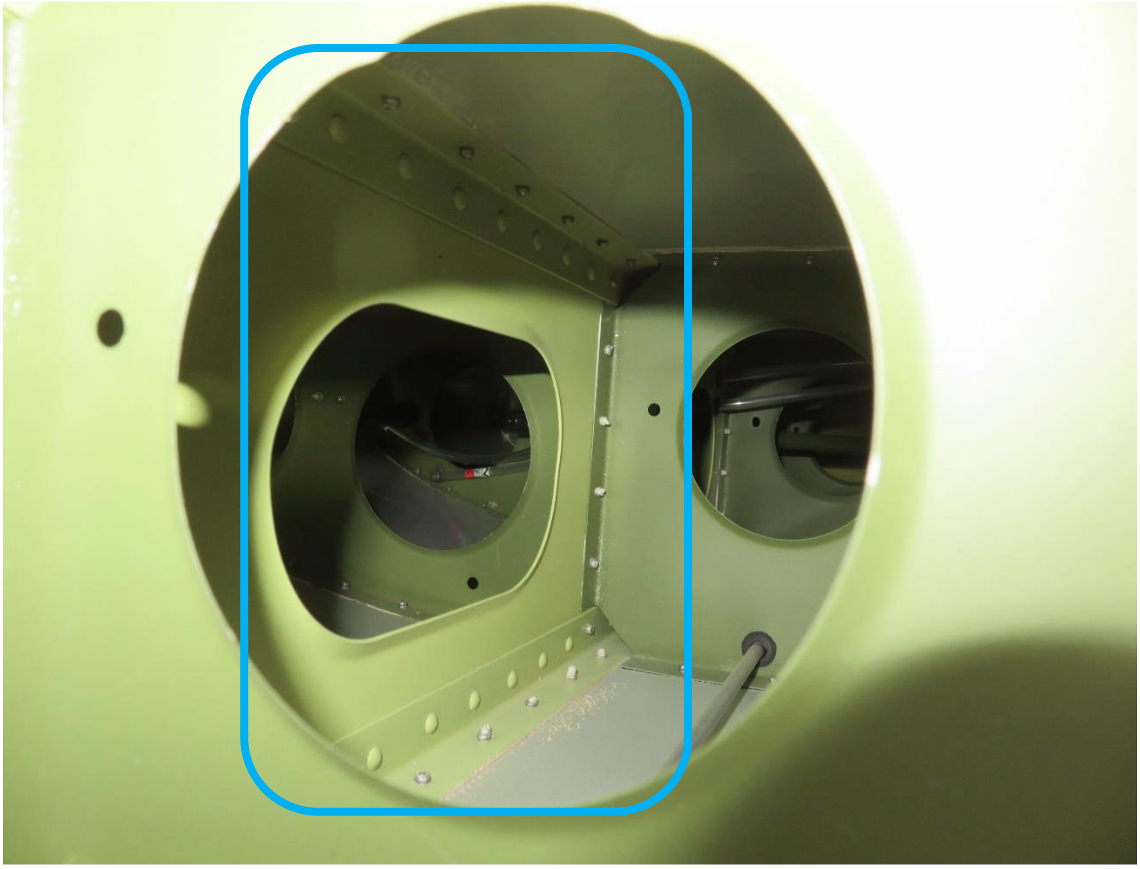

Figure 21: A view of the main spar inside the outer section of the left-wing which failed in-flight.

1.18.4 Thunderstorm Formation and Aviation Hazards

Source: https://www.weather.gov/media/publications/front/11jul-front.pdf

Thunderstorms are one of the most beautiful atmospheric phenomena. As a pilot, however, thunderstorms are one of the most hazardous conditions you can encounter. All thunderstorms can produce severe turbulence, low level wind shear, low ceilings and visibilities, hail, and lightning. Each of these hazards can be difficult to cope with; if all these conditions arrive at once, it can be disastrous. Understanding basic thunderstorm formation and structure can help you make safe decisions. Thunderstorms are formed by a process called convection, defined as the transport of heat energy. Because the atmosphere is heated unevenly, an imbalance can occur which thunderstorms attempt to correct. Three things are needed for convection to be a significant hazard to flight safety: moisture, lift and instability.

Moisture: *Sufficient moisture must be present for clouds to form. Although convection occurs in the atmosphere without visible clouds, think thermals on a warm afternoon, moisture not only is the source of a visible cloud, but also fuels the convection to continue. As the warm air rises, it cools, and the water vapor in the air condenses into cloud droplets. The condensation releases heat, allowing the rising air to stay buoyant and continue to move upward.*

Lift: *There are many ways for air to be lifted in the atmosphere. Convection, or buoyancy, is one method. Other meteorological methods include fronts, low pressure systems, interactions between thunderstorms, and interactions between the jet stream and the surface weather systems. Air also can be lifted by mechanical lift, such as when it is forced up and over a mountain range. Regardless of how the air is lifted, if the lift is enough to make the air warmer than the surrounding air, convection can continue.*

Instability: *In general, as you increase in altitude, the air temperature cools up to the top of the troposphere. Of course, around fronts, mountains and in shallow layers near the ground, this is not always the case. How fast air cools is a measure of atmospheric stability. Meteorologists refer to this vertical change in temperature as the lapse rate. Outside of extremes, the temperature generally decreases from between 2.7°F - 5.4°F per 1000 feet. If the actual rising air cools slower than the lapse rate, the air remains relatively warm compared to the surroundings, and it continues to rise.*

Hazards Associated with Thunderstorms

It is wise to avoid thunderstorms, as a flight instructor once said, "A thunderstorm is never as bad inside as it looks from the outside - it is worse." Thunderstorms contain many hazards to aviation such as the following:

Lightning: *By definition, all thunderstorms contain lightning. Although the NWS will mention lightning as a hazard in some warning products, lightning is not a criteria used to determine if a thunderstorm is severe. As an aviator, you should be aware that lightning can strike more than 10 miles from a thunderstorm. Lightning strike the ground, another cloud or discharge into clear air.*

Turbulence: *Pilot reports from aircraft encountering thunderstorms have noted up and down drafts exceeding 6 000 feet per minute. Turbulence exceeding the performance capability of most aircraft can be found in and around thunderstorms.*

Wind Shear: *Thunderstorm outflow can cause extreme changes in wind speed and direction near the surface during critical phases of flight. Microbursts are possible with many thunderstorms, as is heavy rain. Often virga and blowing dust on the surface are your only clues to the presence of a microburst.*

Icing: *Because thunderstorms are driven, in part, from the conversion of liquid water to ice, pilots can expect to find airframe icing in all thunderstorms. Although all forms of icing are possible, clear icing, caused by larger drops of supercooled water, is the most common. Ice accumulation can be rapid. Supercooled water and clear icing can extend to great heights and to temperatures as low as -20°C.*

The FAA publication, **Thunderstorm Avoidance Tips** *puts it succinctly: "To rely solely on Air Traffic Control (ATC) as a source for weather avoidance is not entirely prudent. It is the pilot's responsibility to obtain a prefight weather briefing. Any ATC reported weather information, along with periodic contacts with Flight Watch while airborne, will supplement what was learned during the prefight briefing. The ATC reports of precipitation areas are of value because they can give you a global view of what is in the area. Pilots who have onboard weather radar or lightning detection systems can benefit from the big picture that ATC can paint and can use the aircraft's onboard systems to pick the best tactical route to avoid severe weather."*

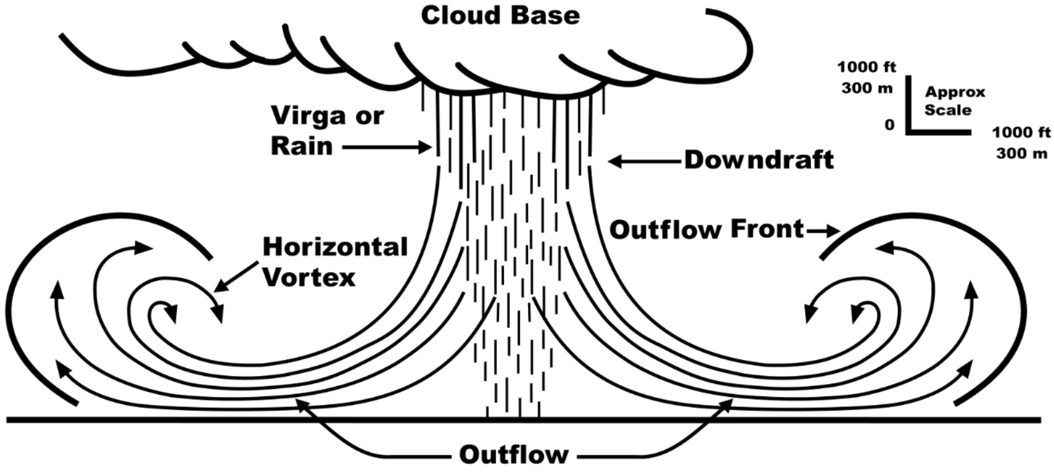

Diagram 3: Illustration of a thunderstorm outflow.

1.19 Useful or Effective Investigation Techniques

1.19.1 No new methods were used.

2. ANALYSIS

2.1 General

From the available evidence, the following analysis was made with respect to this accident. This shall not be read as apportioning blame or liability to any organisation or individual.

2.2 Analysis

2.2.1 The Pilot

When encountering threatening turbulence, the pilot must slow down the aircraft to V-a, which is the manoeuvring speed of the aircraft as tabled in the AFM. If the situation worsens or if the pilot does not feel comfortable, he or she could lower the V-a speed further but should ensure the aircraft does not encounter sluggish/mushy flight controls. For the aircraft in question, the V-a speed was between 86 knots (159 km/h). It is important to note that the airspeed could fluctuate in turbulence and could exceed the V-a speed.

The accident aircraft, being a "light aircraft" (MTOW 550kg), propelled by force would more easily accelerate than a heavy aircraft. A vertical gust, therefore, imposes more of a load on a lightly loaded aircraft than one that is heavily loaded. Since a lightly loaded aircraft is more easily pushed about by gusts/turbulence, it is logical that such an aircraft must be flown more slowly when encountering potentially dangerous turbulence. Also, the V-a speed decreases as gross weight decreases. This is because the stall speed decreases as the aircraft gets lighter. A vertical gust, either from above or below will cause the aircraft to accelerate vertically (up or down), and such acceleration is expressed in Gs (1G is the acceleration felt due to the force of gravity = 9.806 metres per second). Therefore, the greater the acceleration, the greater the G-load would be on the aircraft. Every aircraft will react differently to a given gust. The primary reason for this is the amount of weight supported by each square metre of the wing area. The greater the wing loading, the more difficult it is for a gust to accelerate the aircraft, and vice versa.

A pilot encountering turbulence has three options: (i) change altitude, (ii) alter course, (iii) or ride out the turbulence. Certain pilots have the tendency to ride out the turbulence with aggressive flight control inputs, which would worsen the situation because the manoeuvring loads, the G-forces created, combined with the gust loads create a greater total load(s). To minimise the effect on the aircraft, it is suggested that the pilot maintains a level flight attitude by going through the flow instead of against it to reduce the strain on the aircraft structure.

2.2.2 Portable GPS Download

There were 45 different flight tracks (active track logs) on the GPS unit. Each of these track logs represented a flight (meaning there was a take-off and a landing), except for the accident flight, of which the data is contained in this report.

For most of the accident flight, the aircraft was being flown in a north-easterly direction on a track of approximately 033° (true heading). The pilot then commenced with a right turn towards a south-westerly direction, which was opposite to his inbound heading. The pilot could have decided, at this stage of the flight, to return to his departure aerodrome.

It was noted that the maximum speed (GPS speed, which is ground speed) recorded during the inbound flight was captured at 114 kt (211 km/h). The average speed for the duration of the flight was 91 kt (168 km/h) and the average speed during the right turn was 93 kt (173 km/h). This speed was from the time the pilot commenced with the right turn (change of heading was observed) until the GPS recording stopped, which was while the aircraft was still in the right turn.

Page 2-5 of the AFM states (reference page 24 of this report) next to the V-no airspeed, which is the Maximum Structural Cruising Speed at 103 kt: ***"Do not exceed this speed, with exception of flight in smooth air, and even then, only with increased caution."*** And, next to the V-a airspeed, which is the Manoeuvring Speed at 86 kt: ***"Do not make full or abrupt control movements above this speed, because under certain conditions the aircraft may be <u>overstressed</u> by full control movement."***

It is known (statements from occupants on-board the ZU-AZY) that turbulent conditions prevailed during the flight, especially as the two aircraft flew over the Bronkhorstspruit Dam. The passenger on-board the ZU-AZY stated that: *“As we were halfway over the dam, the wind started throwing us vigorously at all sides.”*

The ZU-AZY pilot stated that: *“As we started heading in a southerly direction over the ridge, I could see waves on the surface of the dam. As I crossed the ridge, I could feel the turbulence. Once over the crash site I tried to drop my right wing in order to see the site. The turbulence at this point was too severe and I could not complete the manoeuvre to see the site. Every time I turned, it felt as if the turbulence was going to overturn my aircraft.”*

2.2.3 Machine (Aircraft)

According to the AFM Section 2, Limitations, *manoeuvring load factors the maximum positive load factor for the aircraft at +4.0g and the maximum negative load factor at -2.0g*. It was possible that the maximum positive load factor was exceeded when the pilot experienced severe turbulence associated with the outflow front of a thunderstorm that was moving through the east of his location at the time. Figure 7 of the report was taken at 1447Z with the photographer facing an easterly direction; the picture shows a thunderstorm towards the east of the dam at the time.

Although the aircraft was destructed during the accident sequence, it was established that apart from the outer section of the left wing that failed in-flight, the integrity of the aircraft was not compromised. It was also evident that the engine was delivering power on impact as all three propeller blades were severed at their respective roots (flash with the propeller spinner). The right wing had separated from the fuselage during the impact sequence and did not display any structural deformation, which is an indication that the wing loading at the time of the failure of the outer section of the left wing was of a much higher +G load than what was experienced on the right wing. It was further noted that the wing failure occurred at the weakest part of the wing spar design, where only a single right angle stiffener bar was present (see Figures 20 and 21).

2.2.4 Environment

The weather data in Figure 1 was taken an hour and thirty-two minutes prior to the accident flight and more than one hour prior to take-off from FASI. During a period of 1.5 hours, the weather conditions (thunderstorm activity) could change radically in Gauteng area. According to the data obtained from the satellite image that was taken at 1500Z on the day, a thunderstorm was present towards the east of the accident area. This was associated with relatively strong winds as well as turbulence.

The pilot and the passenger in the ZU-AZY aircraft stated that they encountered severe turbulent conditions when they flew over the accident site. The weather conditions towards the south had deteriorated (towards FASI) and the ZU-AZY pilot took a decision to divert to FAKT where they landed safely.

2.2.5 Conclusion

The two pilots intended to engage in a pleasure flight. It is a known meteorological fact that during the summer months, afternoon thunderstorms are very common in Gauteng. Even though they had assessed the prevailing weather conditions prior to the flight and were aware of the thunderstorm activity, the pilots proceeded with the flight.

Once airborne, the pilots deviated from their intended flight route, which would have been towards the south (Fortuna Dam near Balfour) and instead of flying to the south, they decided to fly to the north overhead Bronkhorstspruit Dam with the intention to return to FASI.

It is critical for pilots to know their own limitations as well as the limitation of the aircraft they are flying. Pilots can better understand the limitations of the aircraft they fly through flight envelope, discussed in sub-heading 1.18.2. Although the Pilot's Operating Handbook (POH) and the AFM do not contain a diagram of the flight envelope depicted in Diagram 2, all the required information is contained in the documents (POH and AFM) to compile such a diagram for each aircraft type a pilot flies, which might be multiple types for some pilots. Not being aware of these limitations could result in the pilot exceeding the design limitations of the aircraft, which could cause structural damage and/or structural failure. This might or might not result in the failure the first time such an exceedance occurs, but eventually, could result in a structural failure, followed by the loss of control of the aircraft.

At no time during the flight did the pilot mention to his friend that something was wrong with the aircraft. There was also no distress or Mayday call made by the pilot prior to or at the time of the wing failure.

3. CONCLUSION

3.1 General

From the available evidence, the following findings, causes and contributing factors were made with respect to this accident. These shall not be read as apportioning blame or liability to any organisation or individual.

To serve the objective of this investigation, the following sections are included in the conclusion heading:

- **Findings —** are statements of all significant conditions, events, or circumstances in this accident. The findings are significant steps in this accident sequence, but they are not always causal or indicate deficiencies.
- **Causes —** are actions, omissions, events, conditions, or a combination thereof, which led to this accident.
- **Contributing factors —** are actions, omissions, events, conditions, or a combination thereof, which, if eliminated, avoided or absent, would have reduced the probability of the accident occurring, or would have mitigated the severity of the consequences of the accident. The identification of contributing factors does not imply the assignment of fault or the determination of administrative, civil, or criminal liability.

3.2 Findings

The pilot

3.2.1 The pilot was in possession of a National Pilot Licence (NPL), which was initially issued by the Regulator on 2 September 2018. According to his logbook, he had flown a total of 333.8 hours, of which 48.1 hours were on the aircraft type.

3.2.2 The PIC was issued a valid Class 4 aviation medical certificate with hypertension protocol restriction. The medical certificate had an expiry date of 30 June 2022.

3.2.3 The pilot conducted his type conversion onto the aircraft over the period 30 June to 2 July 2021. During this period, he flew 3.4 hours dual with a flight instructor.

The aircraft

3.2.4 The aircraft was issued an Authority to Fly (ATF) on 21 April 2021 with an expiry date of 30 April 2022.

3.2.5 The aircraft was issued a Certificate of Registration (C of R) on 30 June 2021.

3.2.6 The last annual inspection carried out on the aircraft prior to the accident flight was certified on 7 June 2021 at 515.4 airframe hours. The aircraft had accumulated a further 48.6 airframe hours since the said inspection.

3.2.7 The Certificate of Release to Service (CRS) was issued on 7 June 2021 with an expiry date of 7 June 2022 or at a total of 615.4 hours of flight time, whichever occurs first.

3.2.8 The outer section of the left wing failed in-flight and detached from the aircraft.

3.2.9 The entire left wing (both sections) was recovered from the accident site and was made available for metallurgical examination, which found that the wing was exposed to exceedingly high load conditions in-flight, leading to its failure.

Portable GPS

3.2.10 The portable GPS unit that was on-board the aircraft was recovered from the accident site. The accident flight data was downloaded, as well as several tracks from previous flights.

3.2.11 The GPS data of 45 different flights were downloaded and, on most of these flights, high speeds were recorded. However, these speeds could not be linked to indicated airspeed as they reflect groundspeed.

Environment

3.2.12 According to the eyewitnesses interviewed, a sudden wind from the east, described by one of the witnesses to be a *gale force wind,* was blowing in the area at the time of the flight. This wind was present for approximately 5 to 10 minutes and, thereafter, calmed down.

3.2.13 The ZU-AZY pilot stated that whilst flying over the dam, he encountered extremely turbulent flying conditions, and could see the waves on the water. He was unable to orbit the accident scene as it felt as if the aircraft was going to overturn. The pilot also did not opt to fly back to the take-off aerodrome, but diverted to FAKT.

3.2.14 The turbulence they encountered was supported in a statement by the passenger who was on-board the ZU-AZY aircraft, stating that the wind blew vigorously at the time.

3.3 Probable Cause/s

3.3.1 The pilot lost control of the aircraft following a structural failure of the outer left-wing main spar, located 125cm from the wing tip. The failure was associated with an exceedingly high wing load whilst flying in turbulent conditions, caused by the outflow of a nearby thunderstorm cell.

3.4 Contributory Factors

3.4.1 The two pilots continued with their flight in extremely turbulent conditions. They had the option to change their intended destination or opt to return to their take-off aerodrome, weather permitting.

3.4.2 The pilots were aware of the thunderstorm activity over the Gauteng province at the time, yet they opted to proceed with the flight.

4. SAFETY RECOMMENDATIONS

4.1 General

The safety recommendations listed in this report are proposed according to paragraph 6.8 of Annex 13 to the Convention on International Civil Aviation and are based on the conclusions listed in heading 3 of this report. The AIID expects that all safety issues identified by the investigation are addressed by the receiving States and organisations.

4.2 Safety Message

4.2.1 It is recommended to the Director of Civil Aviation that all flight crew be trained on how to properly understand the flight envelope of each aircraft type they fly or might fly in the future as discussed in sub-heading 1.18.2 of this report. It is also of paramount importance that each pilot knows their limitations when boarding an aircraft with the intention to pilot it.

5. APPENDICES

5.1 Appendix A (GPS data downloaded from the unit for the entire accident flight)
5.2 Appendix B (Metallurgical Report from the Laboratory for Microscope & Microanalysis)

This report is issued by:
Accident and Incident Investigations Division
South African Civil Aviation Authority
Republic of South Africa

Appendix A

Summary		Time		Speed		Elevation			
Points:	144	Elapsed Time:	0:24:52	Avg:	168 km/h	Min:	1604 m	Ascent:	896 m
Distance:	69.5 km	Moving Time:	0:24:52	Avg Moving:	168 km/h	Max:	2413 m	Descent:	805 m
Area:	20.6 sq km	Stopped Time:	0:00:00	Min:	1.3 km/h	Grade:	0.0 %		
				Max:	211 km/h				

Index	Elevation	Leg Distance	Leg Time	Leg Speed	Leg Course	Time	Position
1	1604 m	3 m	0:00:07	1.3 km/h	196.8° true	2021/12/07 16:47:33	S26° 15.297' E28° 23.747'
2	1604 m	31 m	0:00:22	5 km/h	200.8° true	2021/12/07 16:47:40	S26° 15.298' E28° 23.747'
3	1606 m	32 m	0:00:20	6 km/h	216.1° true	2021/12/07 16:48:02	S26° 15.314' E28° 23.740'
4	1616 m	21 m	0:00:12	6 km/h	266.6° true	2021/12/07 16:48:22	S26° 15.328' E28° 23.728'
5	1619 m	44 m	0:00:11	14 km/h	14.5° true	2021/12/07 16:48:34	S26° 15.329' E28° 23.716'
6	1621 m	108 m	0:00:06	65 km/h	15.8° true	2021/12/07 16:48:45	S26° 15.306' E28° 23.723'
7	1622 m	166 m	0:00:06	100 km/h	16.0° true	2021/12/07 16:48:51	S26° 15.250' E28° 23.740'
8	1621 m	246 m	0:00:07	127 km/h	16.3° true	2021/12/07 16:48:57	S26° 15.164' E28° 23.768'
9	1624 m	413 m	0:00:11	135 km/h	20.1° true	2021/12/07 16:49:04	S26° 15.036' E28° 23.809'
10	1663 m	419 m	0:00:11	137 km/h	19.0° true	2021/12/07 16:49:15	S26° 14.827' E28° 23.895'
11	1690 m	391 m	0:00:10	141 km/h	17.9° true	2021/12/07 16:49:26	S26° 14.614' E28° 23.977'
12	1721 m	237 m	0:00:06	142 km/h	7.2° true	2021/12/07 16:49:36	S26° 14.413' E28° 24.049'
13	1743 m	227 m	0:00:06	136 km/h	354.3° true	2021/12/07 16:49:42	S26° 14.286' E28° 24.067'
14	1765 m	181 m	0:00:05	131 km/h	332.7° true	2021/12/07 16:49:48	S26° 14.165' E28° 24.053'
15	1773 m	147 m	0:00:04	132 km/h	307.7° true	2021/12/07 16:49:53	S26° 14.078' E28° 24.003'
16	1776 m	75 m	0:00:02	136 km/h	297.8° true	2021/12/07 16:49:57	S26° 14.029' E28° 23.934'
17	1778 m	197 m	0:00:05	142 km/h	274.6° true	2021/12/07 16:49:59	S26° 14.010' E28° 23.894'
18	1780 m	155 m	0:00:04	139 km/h	256.2° true	2021/12/07 16:50:04	S26° 14.002' E28° 23.776'
19	1795 m	159 m	0:00:04	143 km/h	237.7° true	2021/12/07 16:50:08	S26° 14.022' E28° 23.686'
20	1803 m	117 m	0:00:03	141 km/h	222.5° true	2021/12/07 16:50:12	S26° 14.068' E28° 23.605'
21	1806 m	330 m	0:00:08	149 km/h	210.9° true	2021/12/07 16:50:15	S26° 14.114' E28° 23.557'
22	1822 m	345 m	0:00:08	155 km/h	202.0° true	2021/12/07 16:50:23	S26° 14.267' E28° 23.455'
23	1838 m	386 m	0:00:09	154 km/h	195.0° true	2021/12/07 16:50:31	S26° 14.440' E28° 23.378'
24	1848 m	588 m	0:00:14	151 km/h	194.3° true	2021/12/07 16:50:40	S26° 14.640' E28° 23.318'
25	1854 m	560 m	0:00:13	155 km/h	195.4° true	2021/12/07 16:50:54	S26° 14.948' E28° 23.230'
26	1858 m	562 m	0:00:13	156 km/h	194.1° true	2021/12/07 16:51:07	S26° 15.239' E28° 23.141'
27	1866 m	554 m	0:00:13	153 km/h	200.9° true	2021/12/07 16:51:20	S26° 15.533' E28° 23.059'
28	1885 m	641 m	0:00:15	154 km/h	201.3° true	2021/12/07 16:51:33	S26° 15.811' E28° 22.940'
29	1880 m	383 m	0:00:09	153 km/h	210.9° true	2021/12/07 16:51:48	S26° 16.133' E28° 22.800'
30	1880 m	629 m	0:00:15	151 km/h	216.0° true	2021/12/07 16:51:57	S26° 16.310' E28° 22.681'
31	1884 m	303 m	0:00:07	156 km/h	208.7° true	2021/12/07 16:52:12	S26° 16.584' E28° 22.459'
32	1892 m	441 m	0:00:10	159 km/h	200.1° true	2021/12/07 16:52:19	S26° 16.728' E28° 22.372'
33	1905 m	177 m	0:00:04	160 km/h	182.0° true	2021/12/07 16:52:29	S26° 16.951' E28° 22.281'
34	1906 m	182 m	0:00:04	164 km/h	165.2° true	2021/12/07 16:52:33	S26° 17.046' E28° 22.277'

Index	Elevation	Leg Distance	Leg Time	Leg Speed	Leg Course	Time	Position
34	1906 m	182 m	0:00:04	164 km/h	165.2° true	2021/12/07 16:52:33	S26° 17.046' E28° 22.277'
35	1905 m	233 m	0:00:05	168 km/h	148.3° true	2021/12/07 16:52:37	S26° 17.141' E28° 22.305'
36	1898 m	241 m	0:00:05	174 km/h	131.9° true	2021/12/07 16:52:42	S26° 17.248' E28° 22.379'
37	1894 m	242 m	0:00:05	174 km/h	117.5° true	2021/12/07 16:52:47	S26° 17.335' E28° 22.486'
38	1893 m	292 m	0:00:06	175 km/h	105.0° true	2021/12/07 16:52:52	S26° 17.395' E28° 22.616'
39	1894 m	339 m	0:00:07	174 km/h	95.8° true	2021/12/07 16:52:58	S26° 17.436' E28° 22.785'
40	1896 m	235 m	0:00:05	169 km/h	81.5° true	2021/12/07 16:53:05	S26° 17.455' E28° 22.988'
41	1896 m	236 m	0:00:05	170 km/h	64.9° true	2021/12/07 16:53:10	S26° 17.436' E28° 23.128'
42	1893 m	562 m	0:00:12	169 km/h	57.8° true	2021/12/07 16:53:15	S26° 17.382' E28° 23.256'
43	1904 m	279 m	0:00:06	168 km/h	47.4° true	2021/12/07 16:53:27	S26° 17.221' E28° 23.542'
44	1912 m	462 m	0:00:10	166 km/h	40.3° true	2021/12/07 16:53:33	S26° 17.118' E28° 23.665'
45	1923 m	515 m	0:00:11	168 km/h	34.3° true	2021/12/07 16:53:43	S26° 16.929' E28° 23.845'
46	1927 m	463 m	0:00:10	167 km/h	35.6° true	2021/12/07 16:53:54	S26° 16.700' E28° 24.019'
47	1925 m	417 m	0:00:09	167 km/h	43.3° true	2021/12/07 16:54:04	S26° 16.497' E28° 24.181'
48	1935 m	500 m	0:00:11	164 km/h	43.3° true	2021/12/07 16:54:13	S26° 16.333' E28° 24.353'
49	1955 m	508 m	0:00:11	166 km/h	36.9° true	2021/12/07 16:54:24	S26° 16.137' E28° 24.559'
50	1954 m	467 m	0:00:10	168 km/h	35.4° true	2021/12/07 16:54:35	S26° 15.918' E28° 24.743'
51	1952 m	517 m	0:00:11	169 km/h	40.7° true	2021/12/07 16:54:45	S26° 15.713' E28° 24.906'
52	1945 m	337 m	0:00:07	173 km/h	28.7° true	2021/12/07 16:54:56	S26° 15.501' E28° 25.108'
53	1953 m	384 m	0:00:08	173 km/h	33.3° true	2021/12/07 16:55:03	S26° 15.342' E28° 25.205'
54	1955 m	435 m	0:00:09	174 km/h	42.1° true	2021/12/07 16:55:11	S26° 15.169' E28° 25.332'
55	1969 m	562 m	0:00:12	169 km/h	44.3° true	2021/12/07 16:55:20	S26° 14.995' E28° 25.507'
56	1992 m	452 m	0:00:10	163 km/h	37.8° true	2021/12/07 16:55:32	S26° 14.778' E28° 25.743'
57	2001 m	555 m	0:00:12	166 km/h	32.9° true	2021/12/07 16:55:42	S26° 14.586' E28° 25.909'
58	2021 m	606 m	0:00:13	168 km/h	31.2° true	2021/12/07 16:55:54	S26° 14.335' E28° 26.090'
59	2031 m	522 m	0:00:11	171 km/h	34.7° true	2021/12/07 16:56:07	S26° 14.055' E28° 26.279'
60	2041 m	438 m	0:00:09	175 km/h	40.6° true	2021/12/07 16:56:18	S26° 13.824' E28° 26.457'
61	2046 m	779 m	0:00:16	175 km/h	41.1° true	2021/12/07 16:56:27	S26° 13.645' E28° 26.629'
62	2046 m	671 m	0:00:14	173 km/h	37.7° true	2021/12/07 16:56:43	S26° 13.328' E28° 26.936'
63	2054 m	482 m	0:00:10	174 km/h	36.7° true	2021/12/07 16:56:57	S26° 13.042' E28° 27.183'
64	2073 m	585 m	0:00:12	176 km/h	40.8° true	2021/12/07 16:57:07	S26° 12.834' E28° 27.356'
65	2095 m	652 m	0:00:13	180 km/h	39.1° true	2021/12/07 16:57:19	S26° 12.595' E28° 27.586'
66	2104 m	638 m	0:00:13	177 km/h	37.1° true	2021/12/07 16:57:32	S26° 12.322' E28° 27.833'
67	2142 m	576 m	0:00:12	173 km/h	35.4° true	2021/12/07 16:57:45	S26° 12.048' E28° 28.064'

Index	Elevation	Leg Distance	Leg Time	Leg Speed	Leg Course	Time	Position
68	2172 m	784 m	0:00:16	176 km/h	31.8° true	2021/12/07 16:57:57	S26° 11.795' E28° 28.265'
69	2211 m	609 m	0:00:12	183 km/h	32.8° true	2021/12/07 16:58:13	S26° 11.436' E28° 28.513'
70	2229 m	783 m	0:00:15	188 km/h	32.7° true	2021/12/07 16:58:25	S26° 11.160' E28° 28.711'
71	2243 m	584 m	0:00:11	191 km/h	34.5° true	2021/12/07 16:58:40	S26° 10.805' E28° 28.966'
72	2256 m	1.1 km	0:00:21	190 km/h	36.4° true	2021/12/07 16:58:51	S26° 10.545' E28° 29.164'
73	2276 m	1.0 km	0:00:19	192 km/h	33.7° true	2021/12/07 16:59:12	S26° 10.065' E28° 29.559'
74	2295 m	729 m	0:00:14	187 km/h	33.9° true	2021/12/07 16:59:31	S26° 09.612' E28° 29.896'
75	2300 m	693 m	0:00:13	192 km/h	32.3° true	2021/12/07 16:59:45	S26° 09.286' E28° 30.140'
76	2310 m	752 m	0:00:14	193 km/h	36.2° true	2021/12/07 16:59:58	S26° 08.970' E28° 30.362'
77	2319 m	969 m	0:00:18	194 km/h	37.4° true	2021/12/07 17:00:12	S26° 08.643' E28° 30.629'
78	2354 m	935 m	0:00:17	198 km/h	38.4° true	2021/12/07 17:00:30	S26° 08.228' E28° 30.982'
79	2373 m	499 m	0:00:09	200 km/h	33.6° true	2021/12/07 17:00:47	S26° 07.833' E28° 31.331'
80	2382 m	950 m	0:00:17	201 km/h	32.5° true	2021/12/07 17:00:56	S26° 07.609' E28° 31.497'
81	2410 m	685 m	0:00:12	206 km/h	33.1° true	2021/12/07 17:01:13	S26° 07.177' E28° 31.803'
82	2413 m	878 m	0:00:15	211 km/h	30.0° true	2021/12/07 17:01:25	S26° 06.868' E28° 32.027'
83	2400 m	848 m	0:00:15	203 km/h	28.5° true	2021/12/07 17:01:40	S26° 06.458' E28° 32.291'
84	2368 m	693 m	0:00:12	208 km/h	25.4° true	2021/12/07 17:01:55	S26° 06.056' E28° 32.534'
85	2323 m	688 m	0:00:12	206 km/h	22.5° true	2021/12/07 17:02:07	S26° 05.719' E28° 32.712'
86	2292 m	841 m	0:00:15	202 km/h	23.6° true	2021/12/07 17:02:19	S26° 05.376' E28° 32.870'
87	2250 m	446 m	0:00:08	201 km/h	34.0° true	2021/12/07 17:02:34	S26° 04.961' E28° 33.071'
88	2222 m	1.0 km	0:00:18	203 km/h	36.9° true	2021/12/07 17:02:42	S26° 04.762' E28° 33.221'
89	2152 m	670 m	0:00:12	201 km/h	40.6° true	2021/12/07 17:03:00	S26° 04.325' E28° 33.587'
90	2120 m	701 m	0:00:13	194 km/h	44.6° true	2021/12/07 17:03:12	S26° 04.051' E28° 33.849'
91	2097 m	514 m	0:00:10	185 km/h	44.1° true	2021/12/07 17:03:25	S26° 03.781' E28° 34.144'
92	2085 m	855 m	0:00:17	181 km/h	40.9° true	2021/12/07 17:03:35	S26° 03.583' E28° 34.359'
93	2056 m	550 m	0:00:11	180 km/h	37.1° true	2021/12/07 17:03:52	S26° 03.234' E28° 34.695'
94	2043 m	586 m	0:00:12	176 km/h	33.1° true	2021/12/07 17:04:03	S26° 02.997' E28° 34.893'
95	2041 m	772 m	0:00:16	174 km/h	30.5° true	2021/12/07 17:04:15	S26° 02.733' E28° 35.085'
96	2019 m	402 m	0:00:08	181 km/h	26.7° true	2021/12/07 17:04:31	S26° 02.375' E28° 35.320'
97	2023 m	455 m	0:00:09	182 km/h	29.4° true	2021/12/07 17:04:39	S26° 02.181' E28° 35.429'
98	2010 m	654 m	0:00:13	181 km/h	33.4° true	2021/12/07 17:04:48	S26° 01.967' E28° 35.563'
99	2000 m	737 m	0:00:15	177 km/h	34.2° true	2021/12/07 17:05:01	S26° 01.673' E28° 35.778'
100	1987 m	571 m	0:00:12	171 km/h	36.4° true	2021/12/07 17:05:16	S26° 01.345' E28° 36.027'
101	1976 m	711 m	0:00:15	171 km/h	37.8° true	2021/12/07 17:05:28	S26° 01.097' E28° 36.230'

Index	Elevation	Leg Distance	Leg Time	Leg Speed	Leg Course	Time	Position
101	1976 m	711 m	0:00:15	171 km/h	37.8° true	2021/12/07 17:05:28	S26° 01.097' E28° 36.230'
102	1961 m	524 m	0:00:11	172 km/h	37.9° true	2021/12/07 17:05:43	S26° 00.795' E28° 36.491'
103	1952 m	637 m	0:00:13	176 km/h	37.5° true	2021/12/07 17:05:54	S26° 00.572' E28° 36.684'
104	1958 m	496 m	0:00:10	179 km/h	37.2° true	2021/12/07 17:06:07	S26° 00.299' E28° 36.917'
105	1957 m	697 m	0:00:14	179 km/h	35.8° true	2021/12/07 17:06:17	S26° 00.086' E28° 37.097'
106	1945 m	557 m	0:00:11	182 km/h	32.2° true	2021/12/07 17:06:31	S25° 59.782' E28° 37.342'
107	1933 m	567 m	0:00:11	186 km/h	27.1° true	2021/12/07 17:06:42	S25° 59.528' E28° 37.520'
108	1912 m	612 m	0:00:12	184 km/h	25.7° true	2021/12/07 17:06:53	S25° 59.256' E28° 37.675'
109	1910 m	764 m	0:00:15	183 km/h	28.2° true	2021/12/07 17:07:05	S25° 58.958' E28° 37.834'
110	1897 m	726 m	0:00:14	187 km/h	29.5° true	2021/12/07 17:07:20	S25° 58.595' E28° 38.051'
111	1879 m	623 m	0:00:12	187 km/h	25.1° true	2021/12/07 17:07:34	S25° 58.255' E28° 38.265'
112	1860 m	479 m	0:00:09	192 km/h	30.2° true	2021/12/07 17:07:46	S25° 57.951' E28° 38.424'
113	1837 m	590 m	0:00:11	193 km/h	29.4° true	2021/12/07 17:07:55	S25° 57.728' E28° 38.568'
114	1828 m	591 m	0:00:11	194 km/h	31.9° true	2021/12/07 17:08:06	S25° 57.450' E28° 38.742'
115	1804 m	703 m	0:00:13	195 km/h	32.9° true	2021/12/07 17:08:17	S25° 57.180' E28° 38.929'
116	1794 m	647 m	0:00:12	194 km/h	29.1° true	2021/12/07 17:08:30	S25° 56.861' E28° 39.158'
117	1784 m	589 m	0:00:11	193 km/h	25.6° true	2021/12/07 17:08:42	S25° 56.557' E28° 39.347'
118	1766 m	616 m	0:00:12	185 km/h	26.4° true	2021/12/07 17:08:53	S25° 56.270' E28° 39.499'
119	1743 m	535 m	0:00:11	175 km/h	26.5° true	2021/12/07 17:09:05	S25° 55.973' E28° 39.664'
120	1732 m	864 m	0:00:18	173 km/h	27.8° true	2021/12/07 17:09:16	S25° 55.715' E28° 39.807'
121	1698 m	570 m	0:00:12	171 km/h	24.8° true	2021/12/07 17:09:34	S25° 55.303' E28° 40.048'
122	1688 m	749 m	0:00:16	169 km/h	24.4° true	2021/12/07 17:09:46	S25° 55.024' E28° 40.191'
123	1664 m	512 m	0:00:11	168 km/h	26.0° true	2021/12/07 17:10:02	S25° 54.656' E28° 40.377'
124	1662 m	738 m	0:00:16	166 km/h	30.9° true	2021/12/07 17:10:13	S25° 54.408' E28° 40.511'
125	1670 m	699 m	0:00:15	168 km/h	33.2° true	2021/12/07 17:10:29	S25° 54.067' E28° 40.738'
126	1678 m	330 m	0:00:07	169 km/h	42.4° true	2021/12/07 17:10:44	S25° 53.751' E28° 40.968'
127	1678 m	291 m	0:00:06	174 km/h	56.6° true	2021/12/07 17:10:51	S25° 53.620' E28° 41.101'
128	1675 m	535 m	0:00:11	175 km/h	62.4° true	2021/12/07 17:10:57	S25° 53.534' E28° 41.246'
129	1670 m	339 m	0:00:07	174 km/h	68.8° true	2021/12/07 17:11:08	S25° 53.401' E28° 41.530'
130	1667 m	596 m	0:00:12	179 km/h	73.1° true	2021/12/07 17:11:15	S25° 53.335' E28° 41.720'
131	1657 m	449 m	0:00:09	180 km/h	78.1° true	2021/12/07 17:11:27	S25° 53.242' E28° 42.061'
132	1653 m	353 m	0:00:07	182 km/h	85.9° true	2021/12/07 17:11:36	S25° 53.192' E28° 42.325'
133	1654 m	306 m	0:00:06	183 km/h	95.1° true	2021/12/07 17:11:43	S25° 53.178' E28° 42.536'
134	1658 m	308 m	0:00:06	185 km/h	105.4° true	2021/12/07 17:11:49	S25° 53.193' E28° 42.718'

135	1662 m	257 m	0:00:05	185 km/h	118.3° true	2021/12/07 17:11:55	S25° 53.237' E28° 42.896'
136	1669 m	206 m	0:00:04	185 km/h	135.9° true	2021/12/07 17:12:00	S25° 53.303' E28° 43.032'
137	1673 m	209 m	0:00:04	188 km/h	154.3° true	2021/12/07 17:12:04	S25° 53.382' E28° 43.117'
138	1677 m	210 m	0:00:04	189 km/h	172.2° true	2021/12/07 17:12:08	S25° 53.484' E28° 43.172'
139	1684 m	206 m	0:00:04	186 km/h	193.9° true	2021/12/07 17:12:12	S25° 53.596' E28° 43.189'
140	1694 m	158 m	0:00:03	190 km/h	216.9° true	2021/12/07 17:12:16	S25° 53.704' E28° 43.159'
141	1704 m	54 m	0:00:01	196 km/h	230.0° true	2021/12/07 17:12:19	S25° 53.772' E28° 43.102'
142	1705 m	107 m	0:00:02	193 km/h	230.2° true	2021/12/07 17:12:20	S25° 53.790' E28° 43.077'
143	1684 m	147 m	0:00:03	177 km/h	236.5° true	2021/12/07 17:12:22	S25° 53.827' E28° 43.028'
144	1622 m					2021/12/07 17:12:25	S25° 53.871' E28° 42.954'

Appendix B

COMPILED BY:	LABORATORY FOR MICROSCOPY & MICROANALYSIS	PAGE 1 OF 14
	FAILURE ANALYSIS REPORT: MAIN WING ASSEMBLY, EVEKTOR SPORT STAR, AIRCRAFT ZU-EIJ	DOCUMENT NUMBER FA-003-04-20
COMPILED FOR: SACAA (AIID)		DATE 2021-12-15 / ISSUE 1

ITEM: **LEFT-HAND WING ASSEMBLY, EVEKTOR SPORT STAR, AIRCRAFT ZU-EIJ**

1. BACKGROUND INFORMATION

1.1. Selected components from the failed left-hand wing assembly (Photo 2) originating from an Evektor Sport Star Light Sport Aircraft (LSA), registration ZU-EIJ (Photo 1), serial no 2006-0714, were submitted to determine the most probable contributary factor/s towards failure in flight.

1.2. The relevant aircraft was involved in an accident resulting in one fatality (Photo 3).

Photo 1: File Photo, ZU-EIJ[1]


Photo 2: Supplied components, as found (digital)

[1] Courtesy www.JetPhotos.com

Photo 3: Accident site, ZU-EIJ[2]

1.3. This report is divided into the following sections:

2. APPLICABLE DOCUMENTS

(a) Evektor Sport Star IPC
(b) Evektor Aerotechnik Technical Drawings

3. DEFINITIONS

(a)	OEM	Original Equipment Manufacturer
(b)	FEGSEM	Field Emission Gun Scanning Electron Microscope
(c)	FOD	Foreign Object Damage
(d)	EDS	Energy Dispersive X-ray Analysis
(e)	SACAA	South African Civil Aviation Authority
(f)	AIID	Accident and Incident Investigations Division
(g)	IPC	Illustrated Parts Catalogue
(h)	LH	Left-Hand
(i)	RH	Right-Hand
(j)	LE	Leading Edge
(k)	TE	Trailing Edge

[2] Courtesy SACAA/AIID

4. PERSONNEL

(a) The investigative member and compiler of this report is [redacted] ID number [redacted] is a qualified Physical Metallurgist (H.N.Dip. Metallurgical Engineering, Tech. PTA, ECSA Registration: Prof. Eng. Tech. No 201670194), Radiation Protection Officer (RPO, NNR, No 281) and Aircraft Accident Investigator (SCSI).

5. APPARATUS AND METHODOLOGY

(a) The methodology included visual inspection of the affected part/s, sample preparation and Light-Stereo- and FEGSEM/EDS analysis.

6. INVESTIGATION RESULTS

6.1. Visual Inspection

Note 1: *Only the supplied parts were considered.*

The visual inspection of the main wing center section damages revealed no clear indication/s of pre-impact fracture initiation/s (Photo 4, red dashed circles) and can be attributed to overload conditions experienced on impact.

The visual inspection of the supplied LH main wing revealed a disparity in impact damages (Photo's 2 and 3) between the inboard and the outboard sections.

The damages suggest in-flight separation of the outboard section prior to impact with the primary fracture line initiating at the LE at 1666mm and exiting at the TE at 1340mm (Diagrams 1, 2 and 3; red line) as measured from the outer LH wing tip.

The induced overload unto the outboard section as indicated (Diagram 1, red arrow) resulted in a bending moment (blue arrow) and is consistent with an exceedingly high wing-load (+G) imposed during flight.

The fracture initiated between stations 8 and 9 (Diagrams 2 and 3, red line) and exited at the TE between the inboard flap and outboard aileron positions.

The LH main wing inner spar assembly fractured at positions A and B (Photo 5) between stations 8 and 9 (Diagram 3, red lines). The primary fracture initiated outboard from both the lower and upper spar cap stiffener right-angle bars (Diagram 3, red line; Photo 7, red arrow) while proceeding through the oval shaped hole within the spar web (Photo 5, red dashed circle).

The damages to the LH main wing inboard section are consistent with an impact force imposed in the direction as indicated (Diagram 1; Photo 3, yellow dashed arrows).

The primary fracture circumvented the installed wing stiffener between the LH flap and aileron position (Photo 9, red arrows).

The impact damages to the LH aileron pushrod suggest a "full-down" orientation on impact (Photo 10, red dashed circle).

6.2. High Magnification Inspection

Note 2: The primary main wing spar fractures (A and B) were sectioned for microscopy purposes.

The high magnification inspection revealed no clear indication/s of pre-impact fracture initiation/s due to corrosion, fatigue, material- or other discrepancies (Photo's 7 and 8; Fractograph 1).

The fracture surface morphologies confirmed micro-void coalescence with morphologies as a function of the rolling direction of the extruded beams (Fractograph 3) suggesting a tensile, ductile overload condition as the primary contributing factor.

Secondary mechanical damages noted (Fractograph 2) can be attributed to impact and/or post-impact handling.

The main spar cap base material conforms to a 2000 series Aluminium alloy (EDS Result 1).

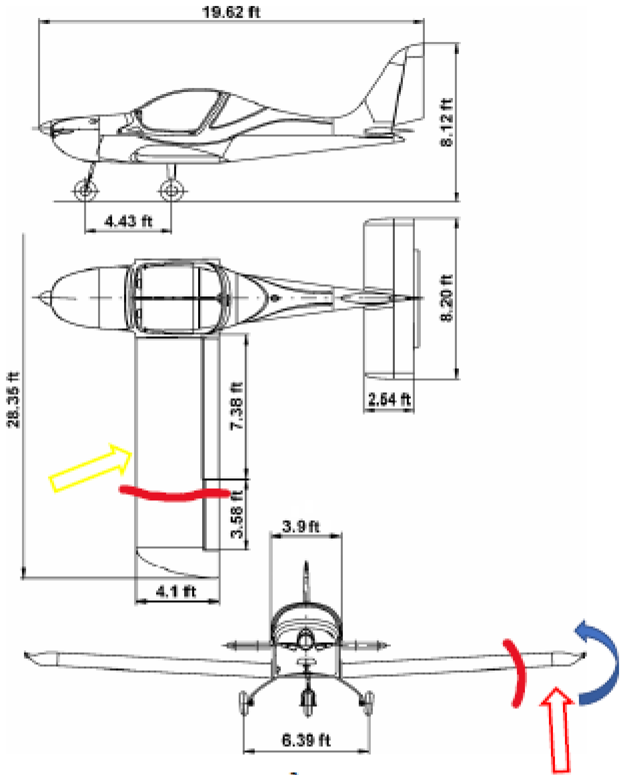

Diagram 1: Aircraft Dimensions[3]

[3] Evektor Spart Star IPC

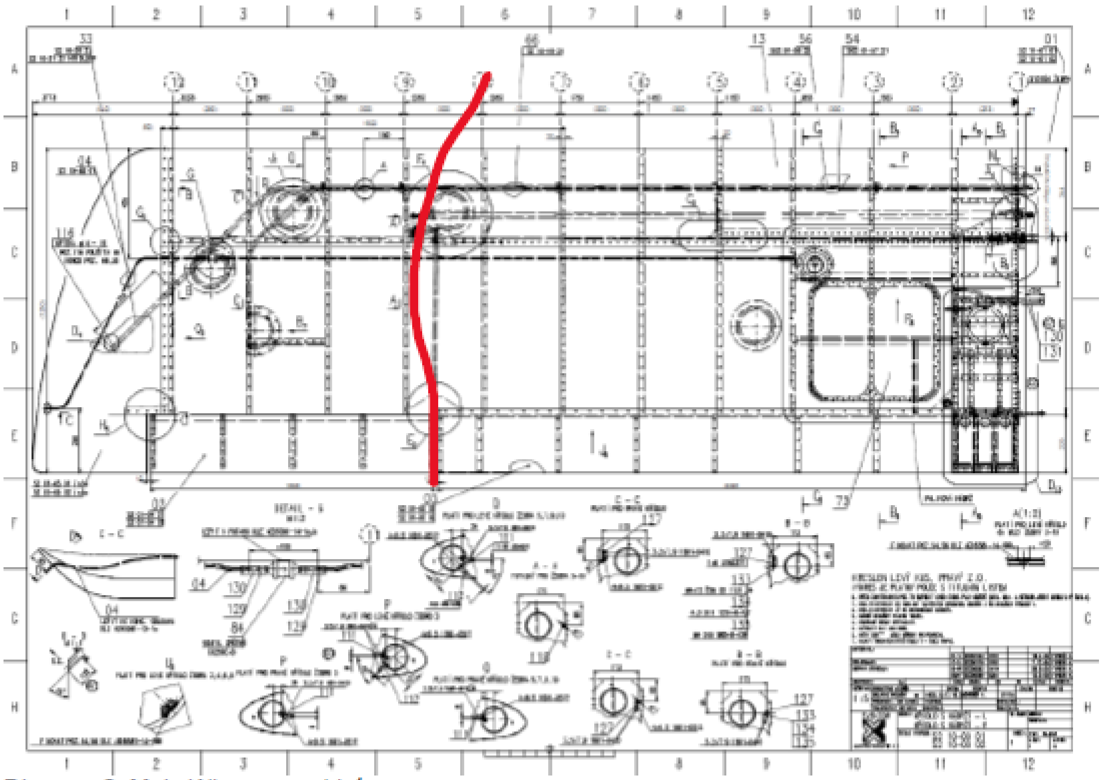

Diagram 2: Main Wing assembly[4]

[4] Courtesy Evektor Aerotechnik

COMPILED BY:	UNIVERSITEIT VAN PRETORIA UNIVERSITY OF PRETORIA YUNIBESITHI YA PRETORIA — LABORATORY FOR MICROSCOPY & MICROANALYSIS	PAGE 6 OF 14
	FAILURE ANALYSIS REPORT: MAIN WING ASSEMBLY, EVEKTOR SPORT STAR, AIRCRAFT ZU-EIJ	DOCUMENT NUMBER FA-003-04-20
COMPILED FOR: SACAA (AIID)		DATE 2021-12-15 / ISSUE 1

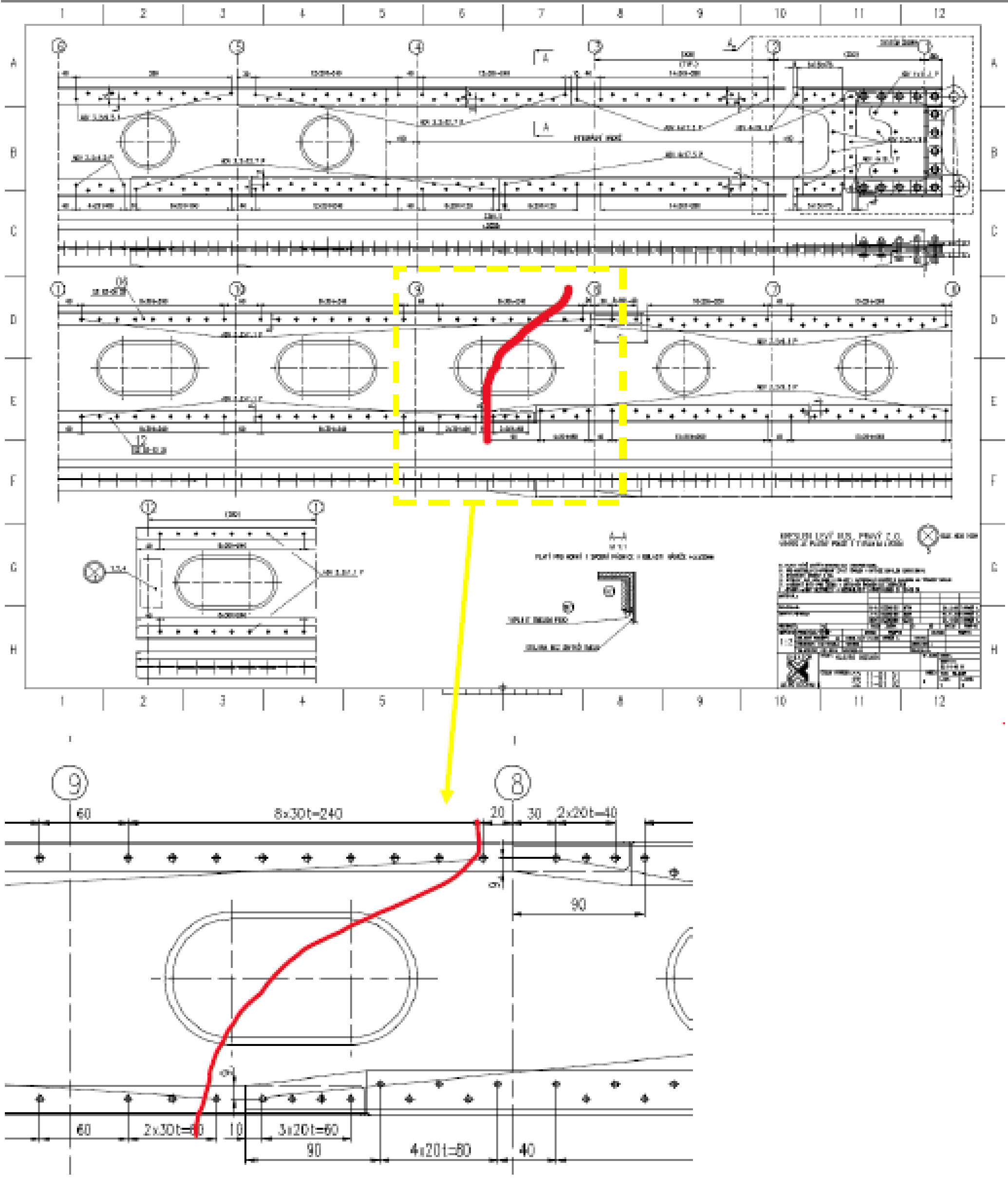

Diagram 3: Main Wing Section/Spar assembly[5]

[5] Courtesy Evektor Aerotechnik

Photo 3: LH wing assembly, as supplied (digital)


Photo 4: Centre section fractures (digital)

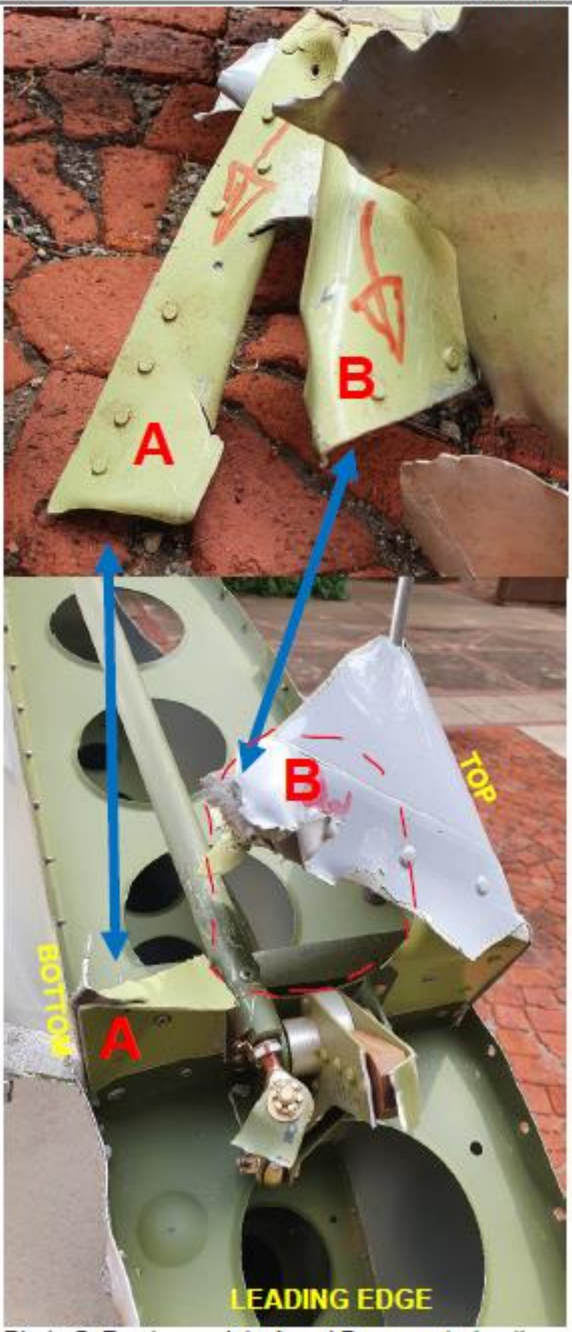

Photo 5: Fracture points A and B, seperated outboard section, LH wing assembly (digital)

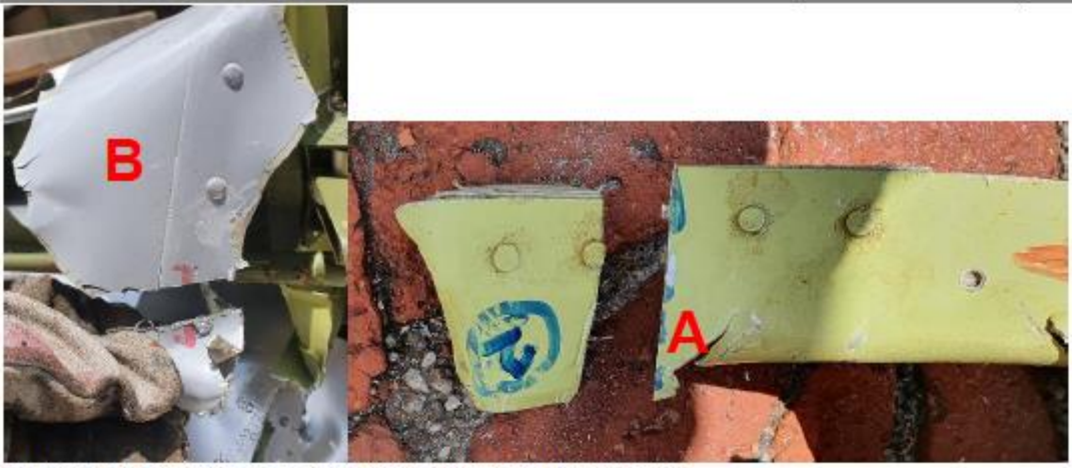

Photo 6: Sectioned fracture locations, outboard section (Stereo)

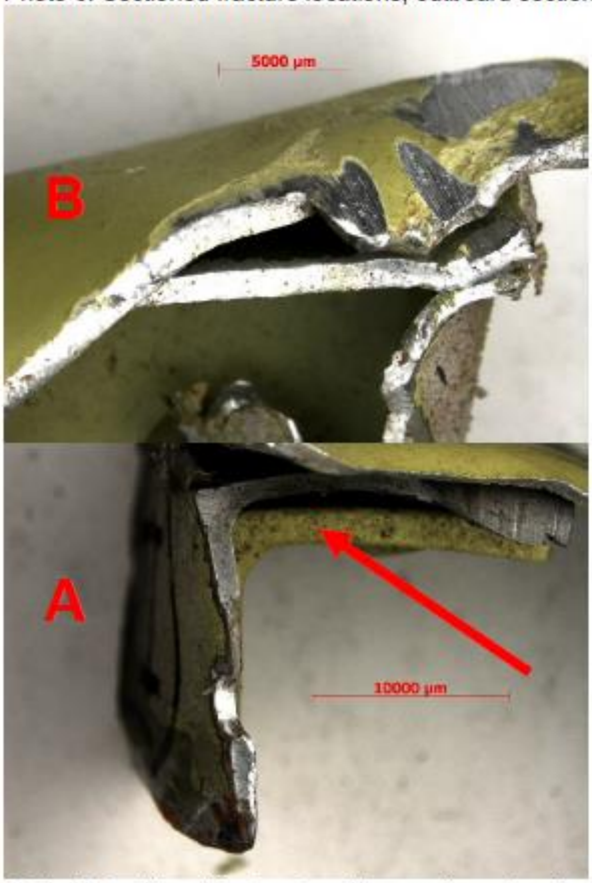

Photo 7: Sectioned fracture locations, outboard section (Stereo)

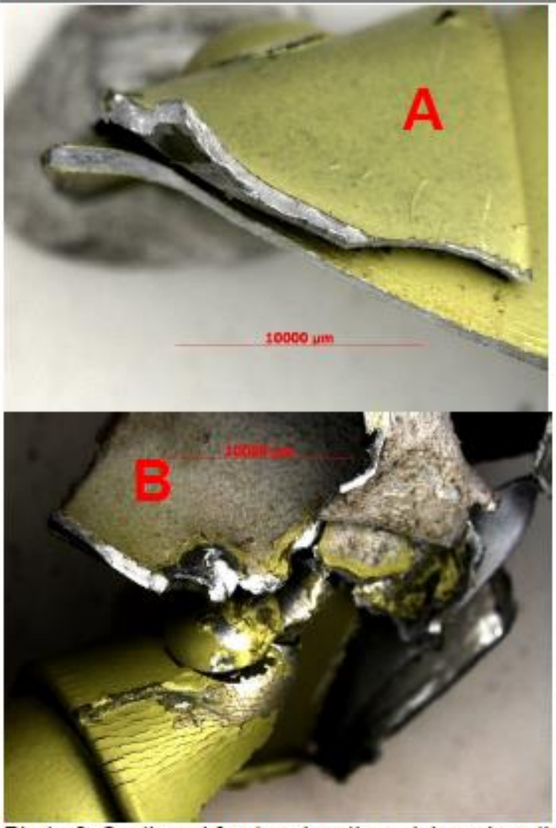

Photo 8: Sectioned fracture locations, inboard section (Stereo)

Photo 9: Fracture progression versus stiffener position (digital)

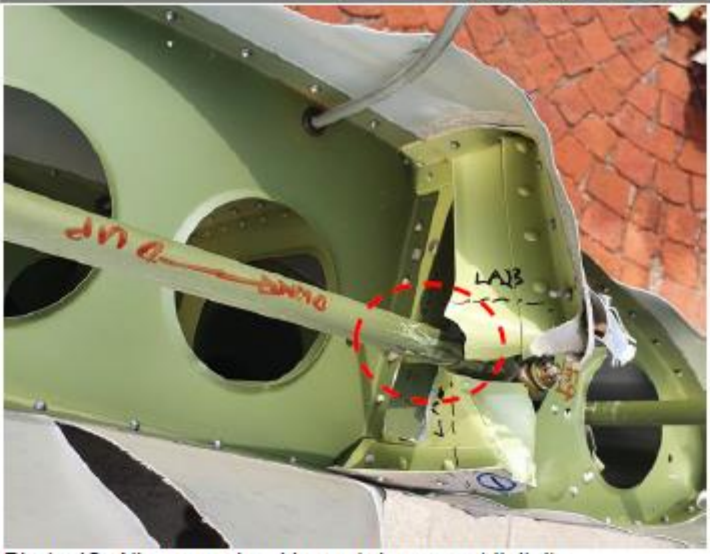

Photo 10: Aileron pushrod impact damages (digital)

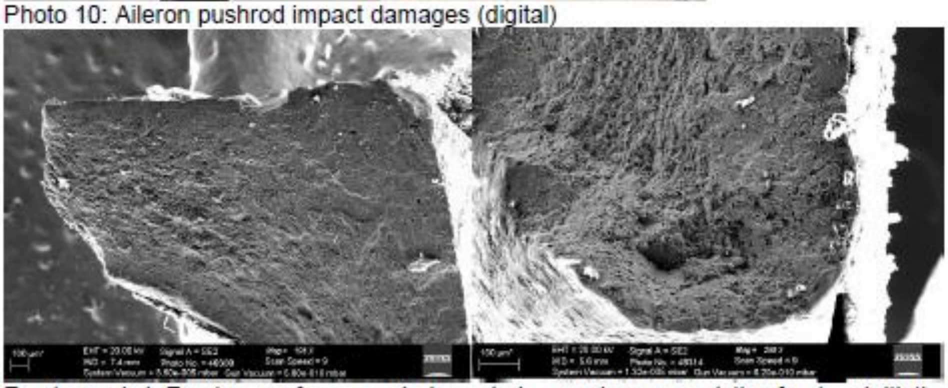

Fractograph 1: Fracture surface morphology shoing no clear pre-existing fracture initiation/s (105-250X, 20kV, SE, FEGSEM)

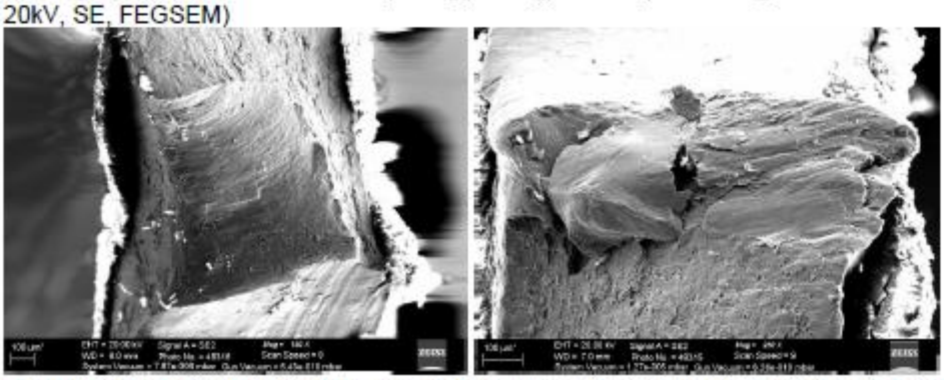

Fractograph 2: Fracture surface morphology showing secondary damages (105-250X, 20kV, SE, FEGSEM)

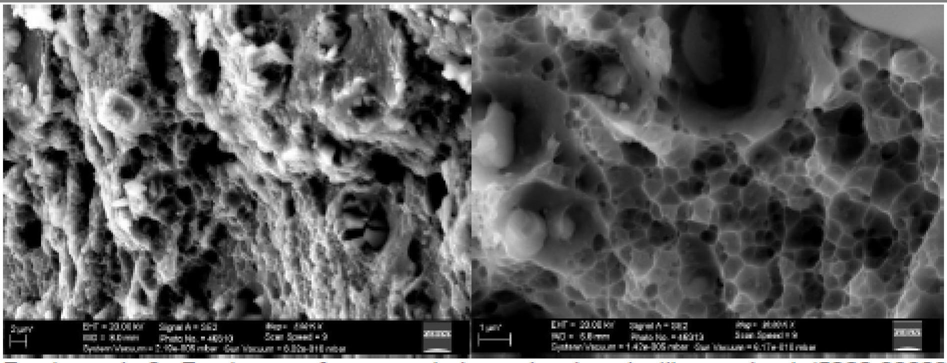

Fractograph 3: Fracture surface morphology showing ductile overload (5000-20000X, 20kV, SE, FEGSEM)

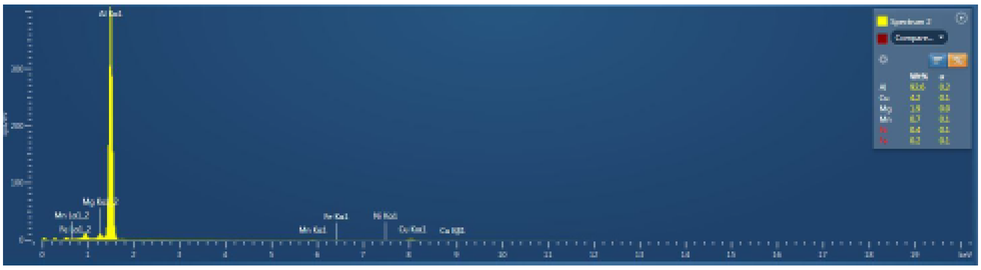

Element	k Ratio	Wt%	Wt% Sigma	Atomic %
Mg	0.01035	1.86	0.05	2.13
Al	0.52264	92.61	0.17	95.38
Mn	0.00408	0.73	0.06	0.37
Fe	0.00122	0.21	0.06	0.11
Ni	0.00205	0.35	0.07	0.17
Cu	0.02344	4.23	0.13	1.85
Total:		100.00		100.00

EDS Result 1: Main wing spar cap base material (Oxford Aztec, 20kV, WD 6.5mm, SE detector)

7. DISCUSSION AND CONCLUSION/S

<u>Note 2</u>: *The conclusions are based on the investigation results obtained from the supplied parts/components and information only. All information supplied to this investigation from other parties are considered factual.*

7.1. The noted disparity in damages within the LH main wing assembly suggest separation of the outboard section due to an exceedingly high wing load condition/s imposed during operation (in-flight breakup).

7.2. The exact cause/s towards this load condition was not determined by this investigation. However, from the supplied accident site photographs (Photo 11), there seems to be a disparity in damages between the LH and RH wings assemblies with emphasis to the outermost sections. This might imply different wing load conditions during the final phase of flight.


Photo 11: RH wing condition, as found[6]

7.3. The results suggest that the LH outboard wing area was exposed to an exceedingly high load condition in the +g region during flight that resulted in the failure of the LH main wing spar assembly as the first in the sequence of events.

7.4. The LH main wing spar caps failed adjacent to and outboard of the end of the second stiffener right angle bars while progressing through the oval spar web hole. The location of the oval spar web hole coincides with the end of the second spar cab stiffener bars suggesting it to be the weakest point within the main wing construction. This investigation could not confirm if the accident aircraft wing construction conforms to the OEM set operational +4g/-2g and/or design limit +6g/-4g specifications[7].

8. RECOMMENDATIONS

8.1. Nonapplicable.

9. DECLARATION

9.1. All digital images have been acquired by the author, unless otherwise stated, and displayed in an un-tampered manner.

[6] Courtesy SACAA
[7] www.evektor.cz